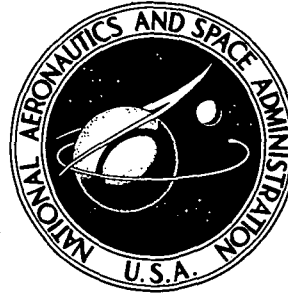


**NASA CONTRACTOR  
REPORT**



**NASA CR-2401**

**NASA CR-2401**

**THE DYADIC DIFFRACTION  
COEFFICIENT FOR A CURVED EDGE**

*by R. G. Kouyoumjian and P. H. Pathak*

*Prepared by*

**THE OHIO STATE UNIVERSITY  
ELECTROSCIENCE LABORATORY**

**Columbus, Ohio 43212**

*for Langley Research Center*



**NATIONAL AERONAUTICS AND SPACE ADMINISTRATION • WASHINGTON, D. C. • JUNE 1974**

1. Report No. NASA CR-2401		2. Government Accession No.		3. Recipient's Catalog No.	
4. Title and Subtitle THE DYADIC DIFFRACTION COEFFICIENT FOR A CURVED EDGE				5. Report Date June 1974	
				6. Performing Organization Code	
7. Author(s) R. G. Kouyoumjian and P. H. Pathak				8. Performing Organization Report No. AR 3001-3	
				10. Work Unit No. 502-33-13-02	
9. Performing Organization Name and Address The Ohio State University  ElectroScience Laboratory Columbus, Ohio 43212				11. Contract or Grant No. NGR 36-008-144	
				13. Type of Report and Period Covered Contractor Report	
12. Sponsoring Agency Name and Address National Aeronautics and Space Administration Washington, D. C. 20546				14. Sponsoring Agency Code	
15. Supplementary Notes  Progress report.					
16. Abstract  A compact dyadic diffraction coefficient for electromagnetic waves obliquely incident on a curved edge formed by perfectly-conducting curved or plane surfaces is obtained. This diffraction coefficient remains valid in the transition regions adjacent to shadow and reflection boundaries, where the diffraction coefficients of Keller's original theory fail. Our method is based on Keller's method of the canonical problem, which in this case is the perfectly-conducting wedge illuminated by plane, cylindrical, conical and spherical waves. When the proper ray-fixed coordinate system is introduced, the dyadic diffraction coefficient for the wedge is found to be the sum of only two dyads, and it is shown that this is also true for the dyadic diffraction coefficients of higher order edges. One dyad contains the acoustic soft diffraction coefficient; the other dyad contains the acoustic hard diffraction coefficient. The expressions for the acoustic wedge diffraction coefficients contain Fresnel integrals, which ensure that the total field is continuous at shadow and reflection boundaries. The diffraction coefficients have the same form for the different types of edge illumination; only the arguments of the Fresnel integrals are different. Since diffraction is a local phenomenon, and locally the curved edge structure is wedge shaped, this result is readily extended to the curved edge. It is interesting that even though the polarizations and the wavefront curvatures of the incident, reflected and diffracted waves are markedly different, the total field calculated from this high-frequency solution for the curved edge is continuous at shadow and reflection boundaries.					
17. Key Words (Suggested by Author(s)) Antennas, Spacecraft and Aircraft, Antennas Applied Electromagnetic Theory			18. Distribution Statement  Unclassified -Unlimited  STAR Category 09		
19. Security Classif. (of this report) Unclassified		20. Security Classif. (of this page) Unclassified		21. No. of Pages 92	22. Price* \$4.00

**Page Intentionally Left Blank**

## CONTENTS

	Page
I. INTRODUCTION	1
II. THE GEOMETRICAL OPTICS FIELD	6
III. THE EDGE DIFFRACTED FIELD	15
IV. DISCUSSION	54
APPENDIX	
I THE CAUSTIC DISTANCE FOR REFLECTION	58
II THE EDGE CAUSTIC DISTANCE	68
III THE PLANES OF INCIDENCE AND REFLECTION	73
IV RECIPROCITY	76
REFERENCES	86

## I. INTRODUCTION

This report is concerned with the construction of a high-frequency solution for the diffraction of an electromagnetic wave obliquely incident on a curved edge in an otherwise smooth, curved, perfectly-conducting surface surrounded by an isotropic, homogeneous medium. The surface normal is discontinuous at the curved edge, and the two surfaces forming the edge may be convex, concave or plane. The solution is developed within the context of Keller's geometrical theory of diffraction<sup>1,2,3</sup> (referred to simply as the GTD henceforth) so the dyadic diffraction coefficient is of interest. Particular emphasis is placed on finding a compact, accurate form of the diffraction coefficient valid in the transition regions adjacent to shadow and reflection boundaries and useful in practical applications.

According to the GTD, a high-frequency electromagnetic wave incident on a curved surface with a curved edge gives rise to a reflected wave, an edge diffracted wave, and an edge excited wave which propagates along a surface ray. Such surface ray fields may also be excited at shadow boundaries of the curved surface. The problem is easily visualized with the aid of Fig. 1, which shows a plane perpendicular to the edge at the point of diffraction  $Q_E$ . The pertinent rays and boundaries are projected onto this plane. To simplify the discussion of the reflected field we have assumed that the local interior wedge angle is  $\leq \pi$ . According to Keller's generalized Fermat's principle, the ray incident on the edge  $Q_E$  produces edge diffracted rays  $ed$  and surface diffracted rays  $sr$ . In the case of convex surfaces the surface ray sheds a surface diffracted ray  $sd$  from each point  $Q$  on its path.



In the present analysis it is assumed that the sources and field point are sufficiently removed from the surface and the boundary ES so that the contributions from the surface ray field can be neglected. The total electric field may then be represented as

$$(1) \quad \bar{E} = \bar{E}^i u^i + \bar{E}^r u^r + \bar{E}^d$$

in which  $\bar{E}^i$  is the electric field of the source in the absence of the surface,  $\bar{E}^r$  is the electric field reflected from the surface with the edge ignored, and  $\bar{E}^d$  is the edge diffracted electric field. The functions  $u^i$  and  $u^r$  are unit step functions which are equal to one in the regions illuminated by the incident and reflected fields and to zero in their shadow regions. The extent of these regions is determined by geometrical optics. The step functions are shown explicitly in Eq. (1) to emphasize the discontinuity in the incident and reflected fields at the shadow and reflection boundaries, respectively. They are not included in subsequent equations for reasons of notational economy.

The diffracted field as defined by Eq. (1) penetrates the shadow region, which according to geometrical optics has a zero field, to account for the nonvanishing fields known to exist there. But the correct high-frequency field must be continuous at the shadow and reflection boundaries; hence the diffracted field must compensate the discontinuities in the incident and reflected fields there. In other words, the diffracted field must provide the correct transition between the illuminated regions and the regions shadowed by the edge.

The high-frequency solution described in the next sections is obtained in the following way. A Luneberg-Kline expansion<sup>4</sup> for the incident field is assumed to be given. The reflected field is expanded similarly and related to the incident field by imposing the boundary condition at the perfectly-conducting surface. Only the leading term, the geometrical optics term, is retained. Next the general form of the leading term in the high-frequency solution for the edge-diffracted electromagnetic field is determined. The wedge (straight edge) geometry is treated first; its dyadic diffraction coefficient is deduced from the asymptotic solution of several canonical problems. Some parameters in this diffraction coefficient are seen to depend on the type of edge illumination. They are determined for an arbitrary incident wavefront by requiring the leading term in the total field to be continuous at the shadow and reflection boundary. It is found that only a slight extension of the solution for the wedge is needed to treat the more general problem posed by the curved edge.

This report is the third in a series of reports dealing with edge diffraction. In the first report<sup>5</sup> the Pauli-Clemmow method of steepest descent was employed in a manner different from that employed by Pauli<sup>6</sup> to obtain a more accurate asymptotic solution for the field diffracted by a wedge. We showed that our generalized Pauli expansion can be transformed term by term into a generalized form of the asymptotic expansion given by Oberhettinger<sup>7</sup>. The leading term in our expansion was found to be more accurate than the leading term in Oberhettinger's expansion; furthermore, our leading term for the diffracted field contains a simple correction factor, which permits

the field to be calculated easily in the transition region. This property is of considerable practical importance, because it enables one to use the geometrical theory of diffraction in the transition regions without introducing a supplementary solution. The correction factors, referred to here as transition functions are simply included with the diffraction coefficient.

In the first report only the scalar problem of plane waves normally incident on the edge of wedge is considered. In the second report<sup>8</sup> this work is extended to obtain a dyadic diffraction coefficient for a perfectly-conducting wedge illuminated by obliquely-incident plane, conical, and spherical waves. By introducing the natural, ray-fixed coordinates, the dyadic diffraction coefficient obtained from each of these canonical problems is reduced to the sum of two dyads. In other words, the matrix formed by the elements of the dyadic diffraction coefficient is a two by two diagonal matrix. The diagonal elements of this matrix are simply the scalar diffraction coefficients,  $D_h$  and  $D_s$ , for the Neumann (hard) and Dirichlet (soft) boundary conditions, respectively. The transition functions appearing in  $D_s$  and  $D_h$  have the same form for the four types of illumination; in each case only a Fresnel integral is involved. However the argument of the Fresnel integral depends upon the type of illumination. Outside of the transition regions these factors are approximately one, and Keller's expressions for the diffraction coefficients are obtained. The asymptotic solutions described in this paragraph help us formulate the solution for a more general type of illumination of the wedge, as noted earlier.

The analysis of wedge diffraction has had a lengthy history. Only a few of the reports and papers have been mentioned thus far. Many of the more important papers on this subject may be found in references 9, 10. A good review of wedge diffraction and the special case of half plane diffraction is given in Chapters 6 and 8 of reference 9. Recently Anluwalia, Boersma, and Lewis have written some papers<sup>11,12,13</sup> of special relevance to the work described here. References 11 and 12 describe high frequency asymptotic expansions for scalar waves diffracted by curved edges in plane and curved screens and reference 13 extends this work to a curved edge in a curved surface. The authors make use of ray coordinates, and some of their results dealing with rays and wavefronts have been helpful in the development of our solution. Nevertheless, there are some noteworthy differences between their solutions and this one, apart from the fact that their problem is scalar instead of the vector problem treated here. Their formulation or ansatz begins with the total field, and the resulting correction of the ordinary GTD solution in the transition region is different from ours. It appears that our result is the more convenient to apply.

## II. THE GEOMETRICAL OPTICS FIELD

The geometrical optics field, which is the sum of the leading terms in the asymptotic expansions for the incident and reflected fields, is a part of our high frequency solution for the edge diffraction. The asymptotic expansions for the incident and reflected fields are presented in this chapter; the results are

not new and so they may be familiar to the reader, but they are included here for the sake of completeness and continuity in the discussion.

Let the smooth, curved perfectly-conducting surface  $S$  be a part of our curved edge structure; this surface is defined by the position vector  $\bar{R}_s(u,v)$ , where  $u$  and  $v$  are the curvilinear surface coordinates with  $\hat{u} \cdot \hat{v} = \hat{u} \cdot \hat{n} = \hat{v} \cdot \hat{n} = 0$  in which the superscript " $\hat{\cdot}$ " denotes a unit vector and  $\hat{n}$  is the unit vector normal to  $S$ , see Fig. 2.

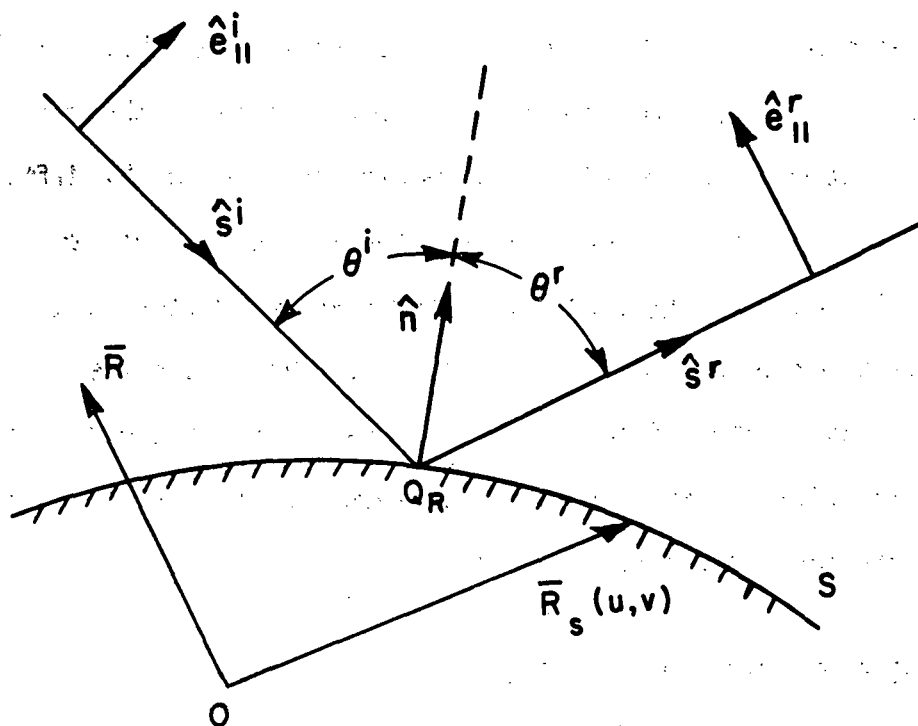


Fig. 2. Geometry associated with the reflection by a curved surface  $S$ .

A high-frequency electromagnetic wave propagating through an isotropic, homogeneous medium is incident on  $S$ . The incident and reflected fields and quantities associated with them are denoted

by the superscripts (or subscripts)  $i$  and  $r$ , respectively. The boundary condition on the electric field at  $S$  is

$$(2) \quad \hat{n}_x[\bar{E}^i(\bar{R}_S) + \bar{E}^r(\bar{R}_S)] = 0.$$

Since we are interested in an asymptotic high frequency solution, the incident and reflected fields are expanded in Luneberg-Kline series for large  $\omega$

$$(3) \quad \bar{E}(\bar{R}) \sim e^{-jk\psi(\bar{R})} \sum_{m=0}^{\infty} \frac{\bar{E}_m(\bar{R})}{(j\omega)^m},$$

where an  $e^{j\omega t}$  time dependence is assumed and  $k = \omega/v_p$  with  $v_p$  the phase velocity of the medium. The electric field is a solution of

$$(4) \quad (\nabla^2 + k^2)\bar{E} = 0$$

subject to the condition that

$$(5) \quad \nabla \cdot \bar{E} = 0.$$

Substituting Eq. (3) into Eqs. (4) and (5) and equating the coefficient of each power of  $\omega$  to zero, one obtains the eikonal equation

$$(6) \quad |\nabla\psi|^2 = 1,$$

together with the transport equations

$$(7a) \quad \frac{\partial}{\partial s} \bar{E}_0 + \frac{1}{2} (\nabla^2 \psi) \bar{E}_0 = 0,$$

$$(7b) \quad \frac{\partial}{\partial s} \bar{E}_m + \frac{1}{2} (\nabla^2 \psi) \bar{E}_m = \frac{v_p}{2} \nabla^2 \bar{E}_{m-1}, \quad m = 1, 2, 3 \dots,$$

whose solutions must also satisfy

$$(8a) \quad \hat{s} \cdot \bar{E}_0 = 0,$$

$$(8b) \quad \hat{s} \cdot \bar{E}_m = v_p \nabla \cdot \bar{E}_{m-1}, \quad m = 1, 2, 3 \dots,$$

where  $\nabla \psi = \hat{s}$  a unit vector in the direction of the ray path, which is normal to the wavefront  $\psi(\bar{R}) = \text{constant}$ , and  $s$  is the distance along the ray path.

We are interested here in the solution at the high frequency limit, where the asymptotic approximation for  $\bar{E}$  reduces to

$$(9) \quad \bar{E}(s) \sim e^{-jk\psi(s)} \bar{E}_0(s)$$

Equation (7a) is readily integrated, and after some manipulation one obtains<sup>14,15</sup>

$$(10) \quad \bar{E}_0(s) = \bar{E}_0(0) \sqrt{\frac{\rho_1 \rho_2}{(\rho_1 + s)(\rho_2 + s)}}$$

in which  $s=0$  is taken as a reference point on the ray path and  $\rho_1$ ,  $\rho_2$  are the principal radii of curvature of the wavefront at  $s=0$ . In Fig. 3  $\rho_1$  and  $\rho_2$  are shown in relationship to the rays and

wavefronts. Employing the Maxwell curl equation  $\nabla \times \vec{E} = -j\omega\mu\vec{H}$ , it follows from Eq. (3) that the leading term in the asymptotic approximation for the magnetic field is

$$(11) \quad \vec{H} \sim Y_c \hat{s} \times \vec{E}$$

where  $Y_c = \sqrt{\epsilon/\mu}$  is the characteristic admittance of the medium, and  $\vec{E}$  is given by Eq. (9).

Employing Eq. (6),

$$d\psi = \nabla\psi \cdot \hat{s} ds = ds;$$

consequently,

$$(12) \quad \psi(s) = \psi(0) + s.$$

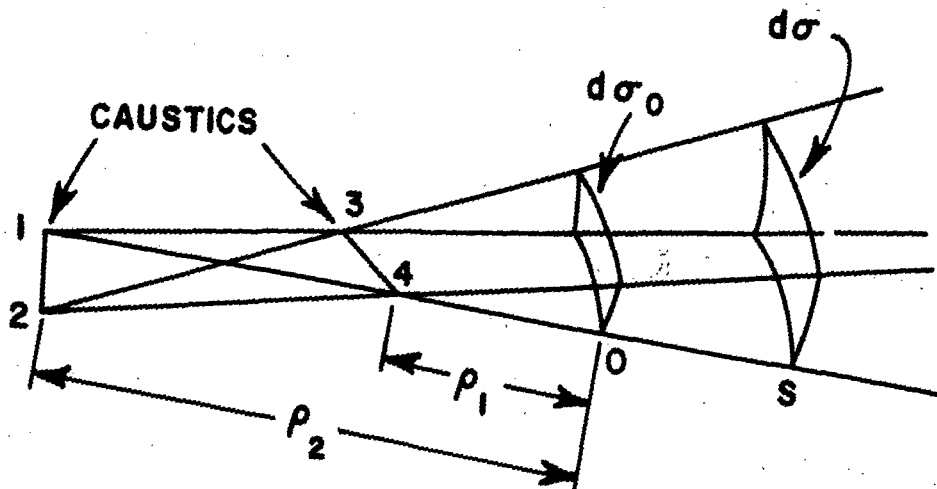


Fig. 3. Astigmatic tube of rays.

From Eqs. (10), (12) and (9) one obtains the leading term in the asymptotic expansion

$$(13) \quad E(s) \sim \bar{E}_0(o) e^{-jk\psi(o)} \sqrt{\frac{\rho_1 \rho_2}{(\rho_1+s)(\rho_2+s)}} e^{-jks},$$

which is recognized as the geometrical optics field; this could have been deduced from classical geometrical optics employing power conservation in the tube of rays shown in Fig. 3.

It is apparent that when  $s = -\rho_1$  or  $-\rho_2$  Eq. (13) becomes infinite so that it is no longer a valid approximation. The congruence of rays at the lines 1-2 and 3-4 of the astigmatic bundles of rays is called a caustic. As we pass through a caustic in the direction of propagation the sign of  $\rho+s$  changes sign and the correct phase shift of  $+\pi/2$  is introduced naturally. Equation (13) is a valid high frequency approximation on either side of the caustic; the field at a caustic must be found from separate considerations<sup>16,17</sup>.

Returning now to our problem of reflection at the perfectly-conducting surface  $S$ , the incident field is known thus the  $\bar{E}_m^i(\bar{R}_o)$  are known. The  $\bar{E}_m^r(\bar{R}_s)$  are found by using the boundary condition. We take the surface  $S$  as the reference point on the reflected ray so  $s = 0$  there; furthermore let us modify our notation for the incident field at point of reflection  $Q_R$  on  $S$ , denoting it by  $\bar{E}^i(Q_R)$ . Now substituting Eq. (3) into Eq. (2) and equating like powers of  $\omega$ ,

$$(14) \quad \hat{n} \times \bar{E}_m^i(Q_R) e^{-jk\psi_i(Q_R)} + \hat{n} \times \bar{E}_m^r(o) e^{jk\psi_r(o)} = 0, \quad m=0,1,2,3,\dots$$

If this equation is to be satisfied for all  $m$ , then

$$(15) \quad \psi_i(Q_R) = \psi_r(o),$$

and since the above is true for every point on  $S$ ,

$$(16a) \quad \hat{u} \cdot \nabla \psi_i(Q_R) = \hat{u} \cdot \nabla \psi_r(o),$$

$$(16b) \quad \hat{v} \cdot \nabla \psi_i(Q_R) = \hat{v} \cdot \nabla \psi_r(o),$$

or

$$(17a) \quad \hat{s}^i \cdot \hat{u} = \hat{s}^r \cdot \hat{u},$$

$$(17b) \quad \hat{s}^i \cdot \hat{v} = \hat{s}^r \cdot \hat{v}.$$

Thus  $\hat{s}^i$  and  $\hat{s}^r$  have the same projection on the plane tangent to  $S$  at  $Q_R$ , which leads us to the law of reflection:

The plane of incidence is defined by the incident ray and the normal to the surface at the point of incidence. The reflected ray lies in the plane of incidence and the angle of reflection  $\theta^r$  equals the angle of incidence  $\theta^i$ , where both angles are measured from the normal to the surface as shown in Fig. 2.

To determine  $\bar{E}_0^r(o)$  it is convenient to introduce the unit vector  $\hat{e}_\perp$  perpendicular to the plane of incidence and the unit vectors  $\hat{e}_\parallel^i$  and  $\hat{e}_\parallel^r$ , which are parallel to the plane of incidence and perpendicular to  $\hat{s}^i$  and  $\hat{s}^r$ , respectively, so that

$$(18) \quad \hat{e}_\perp \times \hat{s} = \hat{e}_\parallel$$

in each case. Then we may set

$$(19) \quad \bar{E}_0 = \hat{e}_\parallel E_{0\parallel} + \hat{e}_\perp E_{0\perp}$$

at the surface. Employing Eqs. (15) and (19) in Eq. (14) we obtain

$$(20) \quad \bar{E}_0^r(o) = \bar{E}_0^i(Q_S) \cdot \bar{R} = \bar{E}_0^i(Q_S) \cdot [\hat{e}_\parallel^i \hat{e}_\parallel^r - \hat{e}_\perp \hat{e}_\perp],$$

where  $\bar{R}$  is the dyadic reflection coefficient. In matrix notation the reflection coefficient has a form familiar for the reflection of a plane electromagnetic wave from a plane, perfectly-conducting surface

$$(21) \quad R = \begin{bmatrix} 1 & 0 \\ 0 & -1 \end{bmatrix}$$

This is not surprising if one considers the local nature of high-frequency reflection, i.e., the phenomena for the most part depends on the geometry of the problem in the immediate neighborhood of  $Q_R$ .

Thus the surface  $S$  can be approximated by its tangent plane at  $Q_R$ , and the wavefront of the incident field by a plane wavefront.

It follows from Eqs. (13), (15) and (20) that the geometrical optics reflected electric field

$$(22) \quad \bar{E}^r(s) = \bar{E}^i(Q_R) \cdot \bar{R} \sqrt{\frac{\rho_1^r \rho_2^r}{(\rho_1^r + s)(\rho_2^r + s)}} e^{-jks}$$

in which  $\rho_1^r$  and  $\rho_2^r$  are the principal radii of curvature of the reflected wavefront at the point of reflection  $Q_R$ . In Appendix I these radii of curvature are found to be a function of the incident wavefront curvature, the aspect of incidence and the curvature of  $S$  at  $Q_R$ . In this appendix it is shown that the expressions for  $\rho_1^r$  and  $\rho_2^r$  can be put into the form

$$(23a) \quad \frac{1}{\rho_1^r} = \frac{1}{2} \left( \frac{1}{\rho_1^i} + \frac{1}{\rho_2^i} \right) + \frac{1}{f_1},$$

$$(23b) \quad \frac{1}{\rho_2^r} = \frac{1}{2} \left( \frac{1}{\rho_1^i} + \frac{1}{\rho_2^i} \right) + \frac{1}{f_2},$$

where  $\rho_1^i$  and  $\rho_2^i$  are the principal radii of curvature of the incident wavefront at  $Q_R$  and

$$\frac{f_1}{2} = \frac{f_2}{2} \left[ \left( \frac{1}{\rho_1^i} - \frac{1}{\rho_2^i} \right), \hat{X}_1 \cdot \hat{U}_1, \hat{X}_1 \cdot \hat{U}_2, \hat{X}_2 \cdot \hat{U}_1, \hat{X}_2 \cdot \hat{U}_2, \theta^i, R_1, R_2 \right],$$

with  $\hat{X}_1$  and  $\hat{X}_2$  unit vectors in the principal directions of the

incident wavefront,  $\hat{U}_1$  and  $\hat{U}_2$  unit vectors in the principal directions of  $S$  at  $Q_R$ , and  $R_1, R_2$  the principal radii of curvature of  $S$  at  $Q_R$ . Equations (23a,b) are reminiscent of the simple mirror formulas of elementary physics; this is particularly true in the case of an incident spherical wave, where  $\rho_1^i = \rho_2^i = s'$  and  $f_1, f_2$  are focal distances independent of the range of the source of the spherical wave.

In principle the geometrical optics approximations can be improved by finding the higher order terms  $\bar{E}_1^r(R), \bar{E}_2^r(R), \dots$  in the reflected field, but in general it is not easy to obtain these from Eqs. (7b), (8b), (14) and (15). Furthermore, these terms do not correct the serious errors in the geometrical optics field resulting from the discontinuities at reflection and shadow boundaries. In the next section we will construct high-frequency approximations for the edge diffracted field which in combination with the geometrical optics field yield a continuous total field.

### III. THE EDGE DIFFRACTED FIELD

The smooth surface  $S$  has a curved edge formed by a discontinuity in its unit normal vector. Points on the edge are defined by the position vector  $\bar{r}$ . When an electromagnetic wave is incident on the edge a diffracted wave emanates from the edge. The leading term in the high frequency approximation for the electric field is assumed to have the form

$$(24) \quad \bar{E}^d(\bar{R}) \sim \frac{e^{-jk\psi_d(\bar{R})}}{\sqrt{k}} \bar{A}(\bar{R}) .$$

Substituting the above expression for  $\bar{E}^d$  into Eqs. (4) and (5), and again equating the coefficient of each power of  $\omega$  to zero, one obtains

$$(25) \quad |\nabla\psi^d| = 1,$$

$$(26) \quad \frac{d}{ds} \bar{A} + \frac{1}{2} (\nabla^2\psi)\bar{A} = 0,$$

$$(27) \quad \hat{s} \cdot \bar{A} = 0,$$

and from the discussion in the preceding section, it follows that

$$(28) \quad \bar{E}^d(s) = \bar{E}^d(0') \sqrt{\frac{\rho\rho'}{(\rho+s)(\rho'+s)}} e^{-jks}$$

in which

$$(29) \quad \bar{E}^d(0') = \frac{\bar{A}(0')}{\sqrt{k}} e^{-jk\psi_d(0')},$$

and  $s$  is the distance along the diffracted ray from a reference point  $0'$  which is not a caustic of the diffracted ray, see Fig. 4.

It is convenient to locate the reference point of the diffracted ray at the edge point  $Q_E$  from which it emanates; however the edge is a caustic of the diffracted field. On the other hand, it is clear that  $\bar{E}^d(s)$  given by Eq. (28) must be independent of the location of  $0'$ , hence

$$\lim_{\rho' \rightarrow 0} \bar{E}^d(0') \sqrt{\rho'} \text{ exists.}$$

Furthermore  $\bar{E}^d(s)$  is proportional to the incident electric field at  $Q_E$ , so we may set

$$(30) \quad \lim_{\rho' \rightarrow 0} \bar{E}^d(O') \sqrt{\rho'} = \bar{E}^i(Q_E) \cdot \bar{D},$$

where  $\bar{D}$  is the dyadic edge diffraction coefficient, which is analogous to the dyadic reflection coefficient of the preceding section.

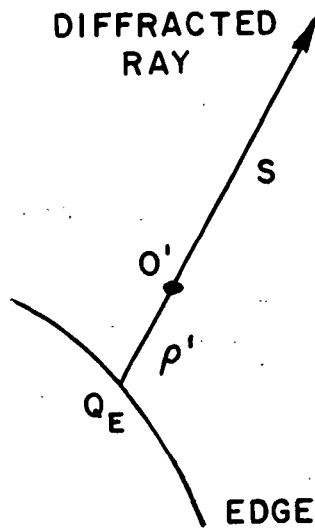


Fig. 4.

Thus the edge diffracted electric field

$$(31) \quad \bar{E}^d(s) \sim \bar{E}^i \cdot \bar{D} \sqrt{\frac{\rho}{s(\rho+s)}} e^{-jks}$$

in which  $\rho$  is the distance between the caustic at the edge and the second caustic of the diffracted ray.

In appendix II it is shown that

$$(32) \quad \frac{1}{\rho} = \frac{1}{\rho_e} + \frac{1}{f} = \frac{1}{\rho_e} - \frac{\hat{n}_e \cdot (\hat{s}' - \hat{s})}{a \sin^2 \beta_0}$$

wherein  $\rho_e^i$  is the radius of curvature of the incident wavefront at  $Q_E$  taken in the plane containing the incident ray and  $\hat{e}$  is the unit vector tangent to the edge at  $Q_E$ ,  $\hat{n}_e$  is the associated unit normal vector to the edge directed away from the center of curvature,  $a > 0$  is the radius of curvature of the edge at  $Q_E$ , and  $\beta_0$  is the angle between the incident ray and the tangent to the edge as shown in Fig. 5a. Equation (32) is seen to have the form of the elementary mirror and lens formulas in which  $f$  is the focal distance. If  $\rho$  is positive, there is no caustic along the diffracted ray path; however the caustic distance  $\rho$  is negative if the (second) caustic lies between  $Q_E$  and the observation point. The diffracted field calculated from Eq. (31) is not valid at a caustic, but as one moves outward from  $Q_E$  along the diffracted ray, a phase shift of  $+\pi/2$  is introduced naturally after the caustic is passed as in the case of the geometrical optics field.

Since the high frequency diffracted field has a caustic at the edge Eq. (31) is not valid there, and we can not impose a condition at  $Q_E$  to determine  $\bar{D}$  in a manner similar to that used to find  $\bar{R}$ . Nevertheless, the matching of the phase functions at the edge

$$(33) \quad \psi_i(Q_E) = \psi_r(Q_E) = \psi_d(Q_E)$$

is a necessary condition, which yields some useful information about the solution. Since the phase is matched at each point on the edge, it follows from Eq. (33) that

$$\hat{e} \cdot \nabla \psi_i(Q_E) = \hat{e} \cdot \nabla \psi_r(Q_E) = \hat{e} \cdot \nabla \psi_d(Q_E),$$

i.e.,

$$(34) \quad \hat{e} \cdot \hat{s}^i = \hat{e} \cdot \hat{s}^r = \hat{e} \cdot \hat{s}.$$

The angle of incidence in this case is  $\beta_0$  defined earlier and shown in Fig. 5a,  $\cos \beta_0 = \hat{e} \cdot \hat{s}^i$ ,  $0 \leq \beta_0 \leq \pi/2$ . The angle of diffraction  $\beta_d$  is the angle between the diffracted ray and the tangent to the edge at  $Q_E$ ;  $\cos \beta_d = \hat{e} \cdot \hat{s}$ ,  $0 \leq \beta_d \leq \pi/2$ . Keller's law of edge diffraction follows from Eq. (34).

The law of edge diffraction: the angle of diffraction  $\beta_d$  is equal to the angle of incidence  $\beta_0$ , so that the diffracted rays emanating from  $Q_E$  form a cone whose half angle is  $\beta_0$  and whose axis is the tangent to the edge. The incident ray and the ray reflected from the surface at  $Q_E$  also lie on the cone of the diffracted rays.

The form of the dyadic diffraction coefficient will be treated next. If an edge-fixed coordinate system is used to describe the components of the incident and diffracted fields, it has been found that the dyadic diffraction coefficient is the sum of seven dyads [18,19]; in matrix form this means that the diffraction coefficient is a  $3 \times 3$  matrix with 7 non-vanishing elements. However from Eqs. (8a) and (27) it is apparent that if a ray-fixed coordinate system were used in place of the edge-fixed coordinate system, the diffraction coefficient would reduce to a  $2 \times 2$  matrix, so that no more than four dyads would be required. A further reduction in the number of dyads can be anticipated if the proper ray-fixed coordinate is chosen. Recall that this kind of simplification is achieved in the case of the dyadic reflection coefficient,

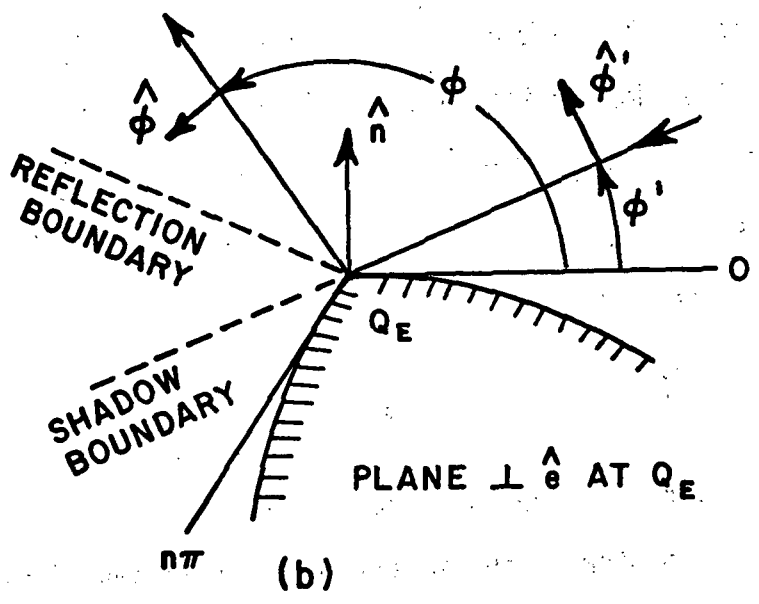
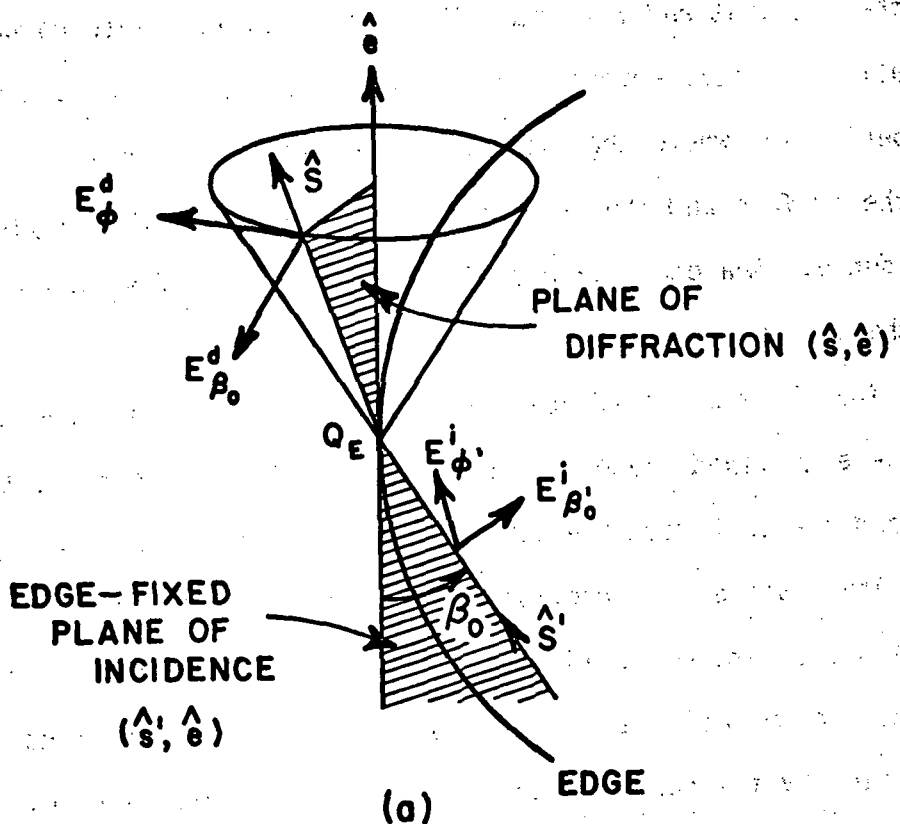


Fig. 5.

if the incident and reflected fields are resolved into components parallel and perpendicular to the planes of incidence and reflection, respectively, where the plane of reflection, which contains the normal to the surface and the reflected ray, coincides with the plane of incidence. Analogous planes of incidence and diffraction can be defined in the present case.

The plane of incidence for edge diffraction, referred to simply as the edge-fixed plane of incidence henceforth, contains the incident ray and the unit vector  $\hat{e}$  tangent to the edge at the point of incidence  $Q_E$ . The plane of diffraction contains the diffracted ray and  $\hat{e}$ . These planes are depicted in Fig. 5; they are azimuthal planes with respect to the polar axis containing  $\hat{e}$ , and their positions can be specified by the angles  $\phi'$  and  $\phi$  shown in Fig. 5b. The unit vectors  $\hat{\phi}'$  and  $\hat{\phi}$  are perpendicular to the edge fixed plane of incidence and the plane of diffraction, respectively. The unit vector  $\hat{s}' \equiv \hat{s}'$  is in the direction of incidence at the edge and the unit vector  $\hat{s}$  is in the direction of diffraction. The unit vectors  $\hat{\beta}'_0$  and  $\hat{\beta}_0$  are parallel to the edge fixed plane of incidence and the plane of diffraction, respectively, and

$$(35a,b) \quad \hat{\beta}'_0 = \hat{s}' \times \hat{\phi}', \quad \hat{\beta}_0 = \hat{s} \times \hat{\phi}.$$

Thus the coordinates of the diffracted ray  $(s, \pi - \beta_0, \phi)$  are spherical coordinates and so are the coordinates of the incident ray  $(s', \beta_0, \phi')$ , except that the incident (radial) unit vector points toward the origin  $Q_E$ .

According to Keller's theory[3] the diffraction coefficient for a curved edge may be deduced from a two-dimensional canonical problem involving a straight edge, where the cylindrical surfaces which form the edge are defined by the boundary curves depicted in Fig. 5b. In the present discussion the edge may be an ordinary edge formed by a discontinuity in the unit normal vector, an edge formed by a discontinuity in surface curvature, or an edge formed by a discontinuity in some higher order derivative of the surface.

Consider the z-components of the electric and magnetic fields in the presence of this surface with an edge

$$(36a) \quad E_z = E_z^i + E_z^r + E_z^d,$$

$$(36b) \quad H_z = H_z^i + H_z^r + H_z^d,$$

they satisfy

$$(37) \quad (\nabla^2 + k^2) \begin{Bmatrix} E_z \\ H_z \end{Bmatrix} = 0$$

together with the soft (Dirichlet) or hard (Neumann) boundary conditions

$$(38,39) \quad E_z = 0 \text{ or } \frac{\partial H_z}{\partial n} = 0,$$

respectively, on the boundary curve and the radiation condition at infinity. The  $\partial/\partial n$  is the derivative along the normal to the boundary curve.

Starting with the high frequency solutions for the z-components of the diffracted field

$$(40) \quad \left. \begin{array}{l} E_z^d \\ H_z^d \end{array} \right\} \sim \frac{e^{-jk\psi(\bar{R})}}{\sqrt{k}} A(\bar{R}),$$

and substituting these into Eq. (37), and employing the methods described earlier, the asymptotic solutions may be put into the form

$$(41) \quad \left. \begin{array}{l} E_z^d \\ H_z^d \end{array} \right\} \sim \left. \begin{array}{l} E_z^i D_s \\ H_z^i D_h \end{array} \right\} \sqrt{\frac{\rho}{s(\rho+s)}} e^{-jks}$$

in which  $D_s$  is referred to as the soft scalar diffraction coefficient obtained when the soft boundary condition is used, and  $D_h$  is referred to as the hard scalar diffraction coefficient obtained when the hard boundary condition is used.

Since

$$(42a) \quad E_z^i = E_{\beta_0}^i \sin \beta_0,$$

$$(42b) \quad H_z^i = Y_c E_{\phi}^i \sin \beta_0,$$

$$(43a) \quad E_z^d = -E_{\beta_0}^d \sin \beta_0,$$

$$(43b) \quad H_z^d = -Y_c E_{\phi}^d \sin \beta_0,$$

with  $1/Y_c = Z_c = \sqrt{\mu/\epsilon}$  the characteristic impedance of the medium,

it follows from Eqs. (41), (42), and (43) that

$$(44) \quad \left. \begin{array}{l} E_{\beta_0}^d \\ E_{\phi}^d \end{array} \right\} = - \left. \begin{array}{l} E_{\beta_0}^i D_s \\ E_{\phi}^i D_h \end{array} \right\} \sqrt{\frac{\rho}{s(\rho+s)}} e^{-jks} ;$$

consequently, the dyadic diffraction coefficient for an ordinary (or higher order) edge is a perfectly-conducting surface can be expressed simply as the sum of two dyads

$$(45) \quad \bar{\bar{D}} = -\hat{\beta}_0' \hat{\beta}_0 D_s - \hat{\phi}' \hat{\phi} D_h$$

to first order. Since  $D_s$  and  $D_h$  are the ordinary scalar diffraction coefficients which occur in the diffraction of acoustic waves which encounter soft or hard boundaries, we see the close connection between electromagnetics and acoustics at high frequencies. Also, it follows that the high frequency diffraction by more general edge structures, and by thin curved wires can be described in the form given by Eqs. (44) and (45).

The balance of this report is concerned with finding expressions for  $D_s$  and  $D_h$  which can be used in the transition regions adjacent to shadow and reflection boundaries in the case of diffraction by an ordinary edge. Recently Keller and Kamnietzky[20] and Senior[21] have obtained expressions for the scalar diffraction coefficients in the case of diffraction by an edge formed by a discontinuity in surface curvature and Senior[22] has given the dyadic (or matrix) diffraction coefficient in an edge-fixed coordinate system. Keller and Kamnietzkey[20] also have given expressions for the scalar diffraction coefficients in the case of higher order edges.

The diffraction by a wedge will be considered first; the straight edge serves as a good introduction to the more difficult subject of diffraction by a curved edge. As noted earlier, the dyadic diffraction

coefficient can be found from the asymptotic solution of several canonical problems, which involve the illumination of the edge by different wavefronts. It is not difficult to generalize the resulting expressions for the scalar diffraction coefficients to the case of illumination by an arbitrary wavefront.

#### A. The Wedge

When a plane, cylindrical, or conical electromagnetic wave is incident on a perfectly-conducting wedge, the solution may be formulated in terms of the components of the electric and magnetic field parallel to the edge; we will take these to be the z-components. In the case of a spherical wave it is convenient to use the z-components of the electric and magnetic vector potentials. These z-components may be represented by eigenfunction series obtained by the method of Green's functions. The Bessel and Hankel functions in the eigenfunction series are replaced by their integral representations and the series are then summed leaving the integral representations. Integral representations for the other field components in the edge-fixed coordinate system are then found from the z (or edge)-components, except in the case of the incident spherical wave, where the integral representations of the field components are obtained from the z-components of the vector potentials. These integrals are approximated asymptotically by the Pauli-Clemow method of steepest descent[23], and the leading terms are retained. The field components are then transformed to the ray-fixed coordinate system described previously. The resulting expression for the diffracted field can be written in the form of Eq. (31) which makes it possible to deduce the dyadic diffraction coefficient  $\bar{D}$ .

The asymptotic solutions outlined in this paragraph are presented in detail in reference [8].

Summarizing the results given in Reference [8]

$$(46) \quad \bar{E}^d(s) \sim \bar{E}^i(Q_E) \cdot \bar{D}(\hat{s}, \hat{s}') A(s) e^{-jks}$$

in which  $A(s)$  describes how the amplitude of the field varies along the diffracted ray;

$$(47) \quad A(s) = \begin{cases} \frac{1}{\sqrt{s}} & \text{for plane, cylindrical and conical wave} \\ & \text{incidence (in the case of cylindrical wave} \\ & \text{incidence, } s \text{ is replaced by } r = s \sin \beta_0, \\ & \text{the perpendicular distance to the edge),} \\ \sqrt{\frac{s'}{s(s'+s)}} & \text{for spherical wave incidence.} \end{cases}$$

It follows from Eq. (32) that  $\rho = \rho_e^i$  for the wedge. In the case of plane, cylindrical and conical waves  $\rho_e^i$  is infinite and in the case of spherical waves  $\rho_e^i = s'$ . The dyadic diffraction coefficient  $\bar{D}(\hat{s}, \hat{s}')$  has the form given in Eq. (45), which supports the assumptions leading to that equation.

If the field point is not close to a shadow or reflection boundary, the scalar diffraction coefficients

$$(49) \quad D_s(\phi, \phi'; \beta_0) = \frac{e^{-j\frac{\pi}{4}} \sin \frac{\pi}{n}}{n\sqrt{2\pi k} \sin \beta_0} \left[ \frac{1}{\cos \frac{\pi}{n} - \cos \left( \frac{\phi - \phi'}{n} \right)} + \frac{1}{\cos \frac{\pi}{n} - \cos \left( \frac{\phi + \phi'}{n} \right)} \right]$$

for all four types of illumination, which is important because the diffraction coefficient should be independent of the edge illumination away from shadow and reflection boundaries where the plane surfaces forming the wedge are  $\phi=0$  and  $\phi = n\pi$ . The wedge angle is  $(2-n)\pi$ ; see

Fig. 5b. This expression becomes singular as shadow or reflection boundaries are approached, which further aggravates the difficulties at these boundaries resulting from the discontinuities in the incident or reflected fields. The above scalar diffraction coefficients have been given by Keller[3].

Grazing incidence, where  $\phi' = 0$  or  $n\pi$  must be considered separately. In this case  $D_s = 0$ , and the expression for  $D_h$  given by Eq. (4) must be multiplied by a factor of  $1/2$ . The need for the factor of  $1/2$  may be seen by considering grazing incidence to be the limit of oblique incidence. At grazing incidence the incident and reflected fields merge, so that one half the total field propagating along the face of the wedge toward the edge is the incident field and the other half is the reflected field. Nevertheless in this case it is clearly more convenient to regard the total field as the "incident" field. The factor of  $1/2$  is also apparent if the analysis is carried out with  $\phi' = 0$  or  $n\pi$ .

Combining Eqs. (31), (45) and (49) it is seen that the diffracted field is of order  $k^{-1/2}$  with respect to the incident and reflected fields. At high frequencies this means that the diffracted field is in general weaker than the incident and reflected fields, at aspects not close to shadow and reflection boundaries.

To simplify the discussion, the wedge angle has been restricted so that  $1 < n \leq 2$ ; however, the solution for the diffracted field may be applied to an interior wedge where  $0 < n < 1$ . The diffraction coefficient vanishes when

---


$$\sin \frac{\pi}{n} = 0;$$

hence for  $n = 1$ , the entire plane,

$n = 1/2$ , the interior right angle,

$n = 1/M$ ,  $M = 3, 4, 5 \dots$ , interior acute angles,

the boundary value problem can be solved exactly in terms of the incident field and a finite number of reflected fields, which may be determined from image theory. Moreover as  $n \rightarrow 0$ , even with the presence of a non-vanishing diffracted field, the phenomenon is increasingly dominated by the incident and reflected fields.

Returning now to the subject of exterior edge diffraction, the total field changes rapidly in the vicinity of shadow and reflection boundaries. In the case of the shadow boundary its behavior is predominantly that of the incident field on the illuminated side, whereas it is that of the diffracted field, emanating from the edge, on the shadow side. For example if the wedge is illuminated by a plane wave perpendicular to its edge, the total field varies from an essentially plane wave behavior to a cylindrical wave behavior in the vicinity of the shadow boundary. These regions of rapid field change adjacent to the shadow and reflection boundaries are referred to as transition regions. In the transition regions the magnitude of the diffracted field is comparable with the incident or reflected field, and since these fields are discontinuous at their boundaries, the diffracted fields must be discontinuous at shadow and reflection boundaries for the total field to be continuous there.

An expression for the dyadic diffraction coefficient of a perfectly-conducting wedge which is valid both within and outside the transition regions[8] is provided by Eq. (45) with

$$(50) \quad D_{\frac{s}{h}}(\phi, \phi'; \beta_0) = \frac{-e^{-j\frac{\pi}{4}}}{2n\sqrt{2\pi k} \sin\beta_0} \times$$

$$\times \left[ \cot\left(\frac{\pi+(\phi-\phi')}{2n}\right) F[kL a^+(\phi-\phi')] + \cot\left(\frac{\pi-(\phi-\phi')}{2n}\right) F[kL a^-(\phi-\phi')] \right]$$

$$\mp \left\{ \cot\left(\frac{\pi+(\phi+\phi')}{2n}\right) F[kL a^+(\phi+\phi')] + \cot\left(\frac{\pi-(\phi+\phi')}{2n}\right) F[kL a^-(\phi+\phi')] \right\} ,$$

where

$$(51) \quad F(X) = 2j\sqrt{X} e^{jX} \int_{\sqrt{X}}^{\infty} e^{-j\tau^2} d\tau$$

in which one takes the principal (positive) branch of the square root, and

$$(52) \quad a^{\pm}(\phi \pm \phi') = 2 \cos^2 \left( \frac{2n\pi N^{\pm} - (\phi \pm \phi')}{2} \right)$$

in which  $N^{\pm}$  are the integers which most nearly satisfy the equations

$$(53a) \quad 2\pi n N^+ - (\phi \pm \phi') = \pi$$

and

$$(53b) \quad 2\pi n N^- - (\phi \pm \phi') = -\pi .$$

The above expression for the soft (s) and hard (h) diffraction coefficients contains a transition function  $F(X)$  defined by Eq. (51),

where it is seen that  $F(X)$  involves a Fresnel integral. The magnitude and phase of  $F(X)$  are shown in Fig. 6, where  $X = kLa$ .

$$(54a) \quad |F(X)| \leq 1 .$$

$$(54b) \quad 0 \leq \text{phase } F(X) \leq \pi/4 .$$

When

$$(55) \quad X > 10,$$

$$F(X) \simeq 1 .$$

If the arguments of the four transition functions in Eq. (51) exceed 10, so the transition functions can be replaced by unity, Eq. (50) reduces to Eq. (49).

$$(56) \quad X = kL a^{\pm}(\phi \pm \phi')$$

in which  $L$  is a distance parameter, which was determined for several types of illumination. It was found that

$$(57) \quad L = \begin{cases} s \sin^2 \beta_0 & \text{for plane wave incidence,} \\ \frac{r r'}{r + r'} & \text{for cylindrical wave incidence,} \\ \frac{ss'}{s + s'} \sin^2 \beta_0 & \text{for conical and spherical wave} \\ & \text{incidence,} \end{cases}$$

where the cylindrical wave of radius  $r'$  is normally incident on the edge, and  $r$  is the perpendicular distance of the field point from the edge. A more general expression for  $L$ , valid for an arbitrary wavefront incident on the straight edge, will be determined later.

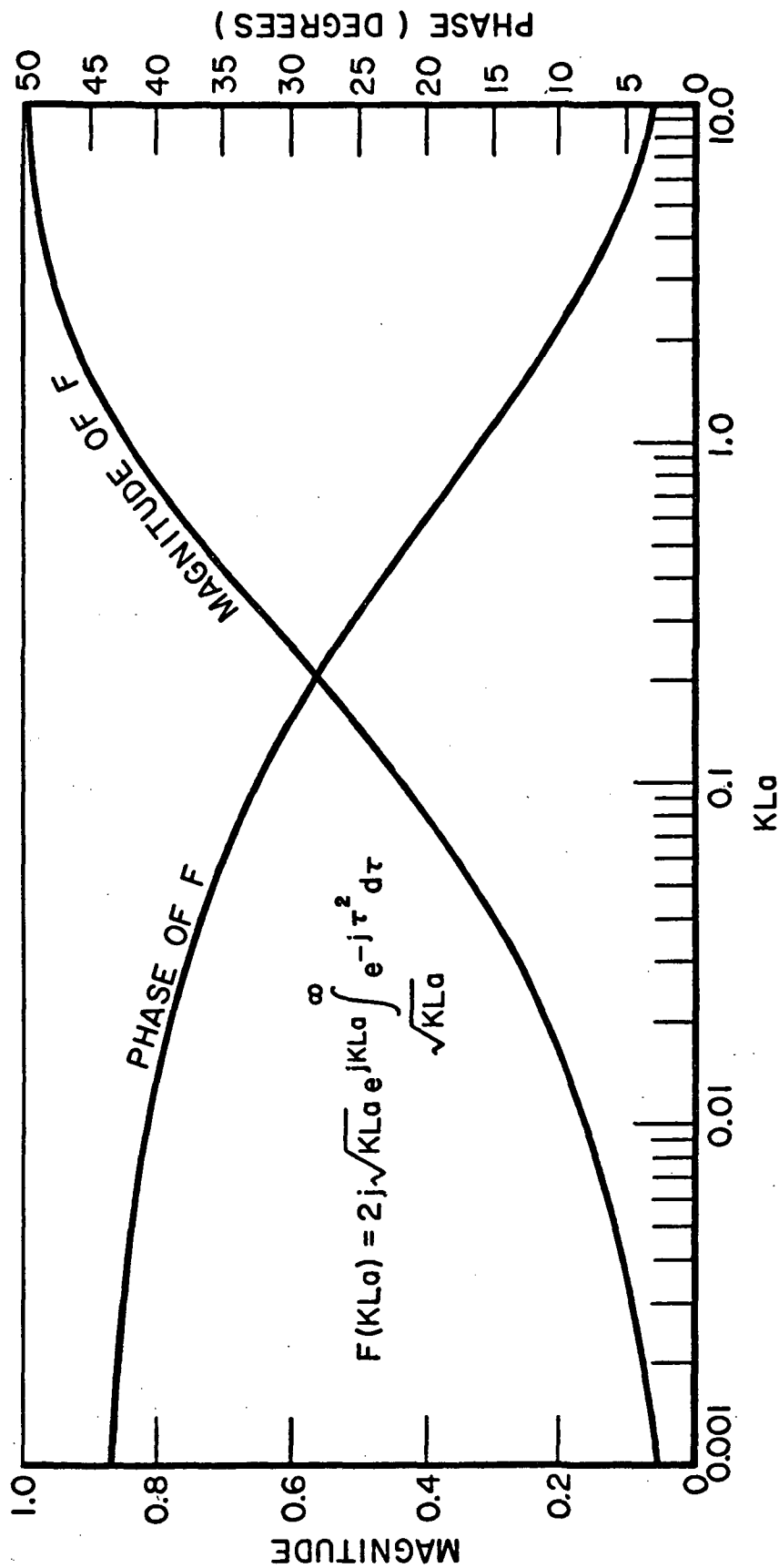


Fig. 6. Transition function.

The largeness parameter in the asymptotic approximation used to find  $D_{\frac{\sigma}{h}}$  is  $kL$ . For incident plane waves the approximation has been found to be accurate if  $kL > 1.0$ , unless  $n$  is close to one, then  $kL$  should be  $> 3$ .

$a^{\pm}(\phi \pm \phi')$  is a measure of the angular separation between the field point and a shadow or reflection boundary. The + and - superscripts are associated with the integers  $N^+$  and  $N^-$ , respectively, which are defined by Eqs. (53a,b). For exterior edge diffraction  $N^+ = 0$  or  $1$  and  $N^- = -1, 0$  or  $1$ . The values of  $N^{\pm}$  as functions of  $n$  and  $\beta = \phi \pm \phi'$  are depicted in Figs. 7a and 7b; these integers are particularly important near the shadow and reflection boundaries shown as dotted lines in the figures. It is seen that  $N^{\pm}$  do not change abruptly with aspect  $\phi$  near these boundaries, which is a desirable property. The trapezoidal regions bounded by the solid straight lines represents the permissible values of  $\beta$  for  $0 \leq \phi, \phi' \leq n\pi$  with  $1 \leq n \leq 2$ .

At a shadow or reflection boundary one of the cotangent functions in the expression for  $D_{\frac{\sigma}{h}}$  given by Eq. (50) becomes singular; the other three remain bounded. Even though the cotangent becomes singular, its product with the transition function will be shown to be bounded. However let us first note the location of the boundary at which each cotangent becomes singular; this information is presented compactly in Table 1. The locations of the shadow and reflection boundaries when only one surface of the wedge is illuminated and when both surfaces of the wedge are illuminated are shown in Figs. 8a, b, c below Table 1.

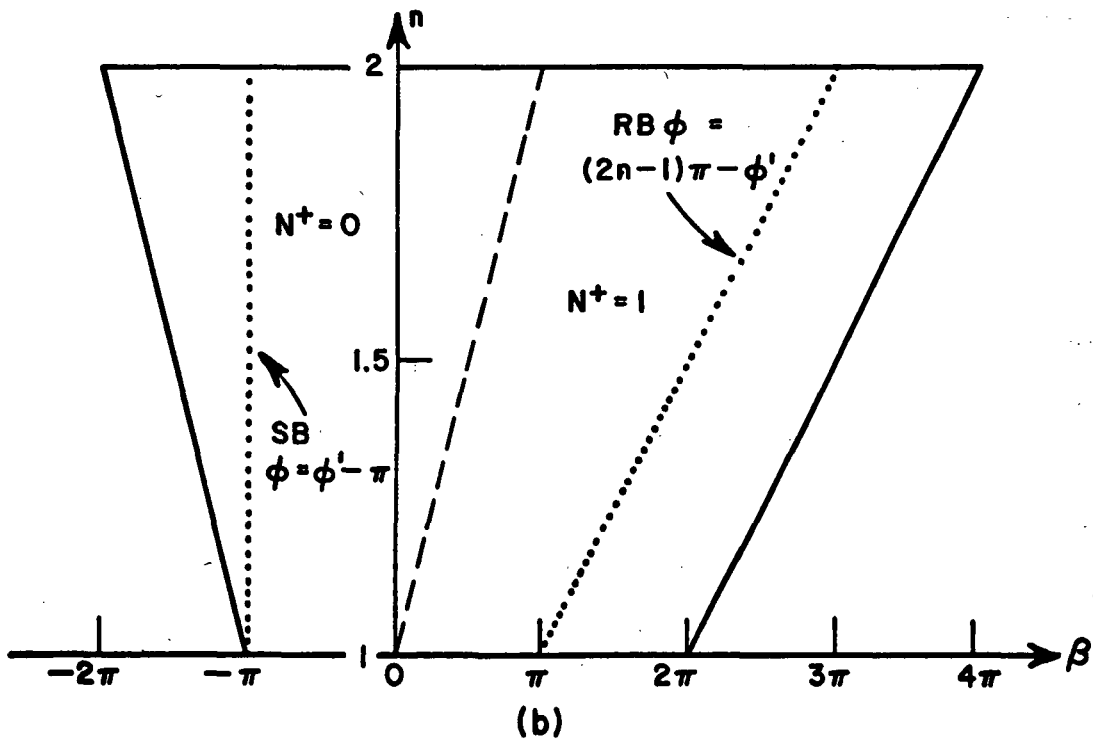
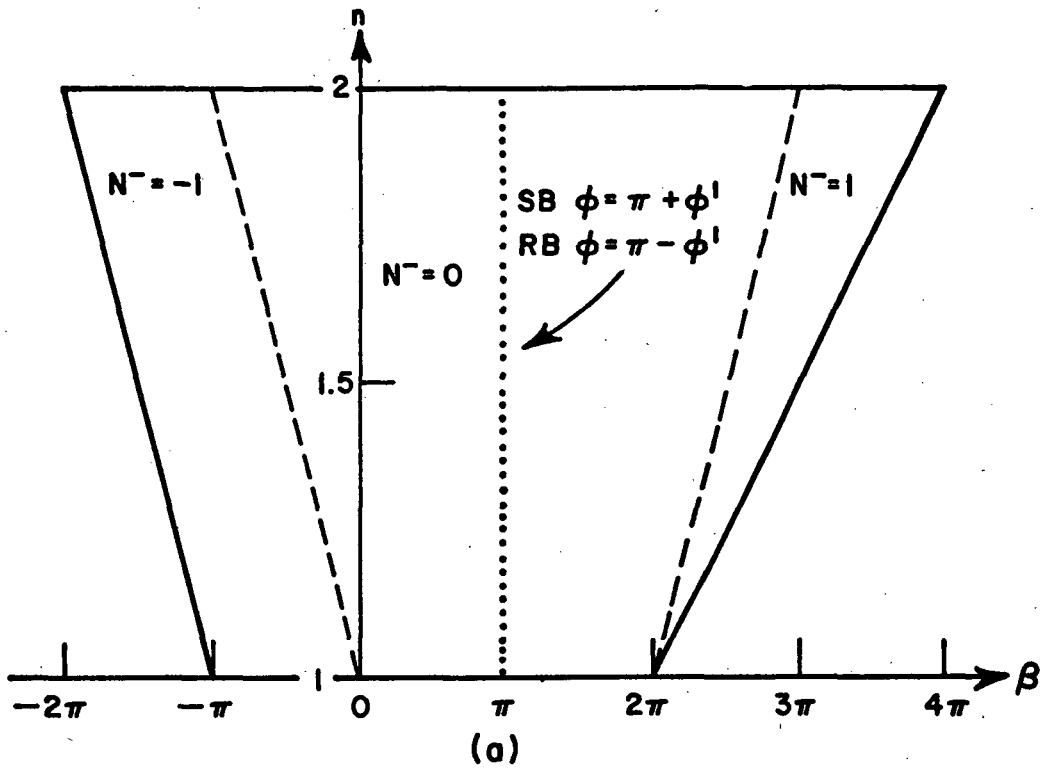


Fig. 7.  $N^+$ ,  $N^-$  as functions of  $\beta$  and  $n$ .

TABLE 1

	The cotangent is singular when	value of N at the boundary
$\cot\left(\frac{\pi+(\phi-\phi')}{2n}\right)$	$\phi = \phi' - \pi$ , a SB surface $\phi=0$ is shadowed	$N^+ = 0$
$\cot\left(\frac{\pi-(\phi-\phi')}{2n}\right)$	$\phi = \phi' + \pi$ , a SB surface $\phi=n\pi$ is shadowed	$N^- = 0$
$\cot\left(\frac{\pi+(\phi+\phi')}{2n}\right)$	$\phi = (2n-1)\pi - \phi'$ , a RB reflection from surface $\phi=n\pi$	$N^+ = 1$
$\cot\left(\frac{\pi-(\phi+\phi')}{2n}\right)$	$\phi = \pi - \phi'$ , a RB reflection from surface $\phi=0$	$N^- = 0$

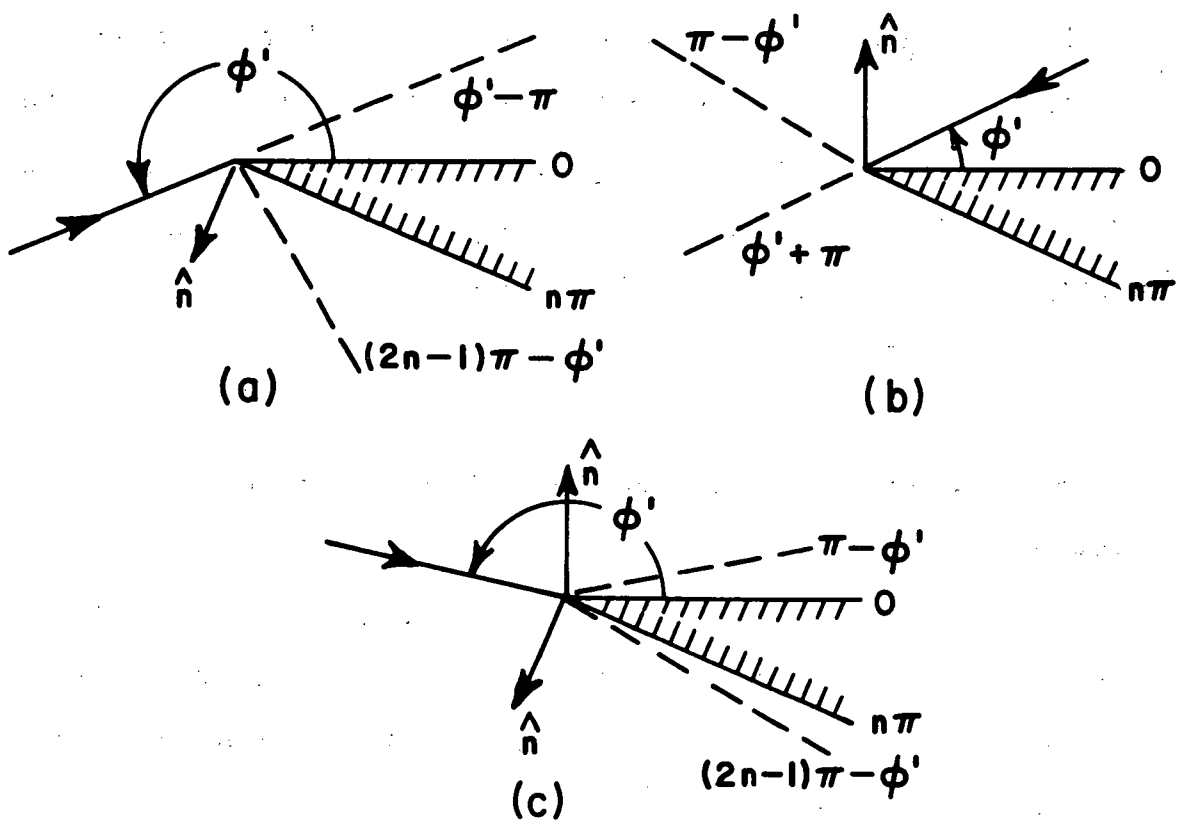


Fig. 8. Shadow and reflection boundaries for different angles of incidence  $\phi'$ .

Since discontinuity in the geometrical optics field at a shadow or reflection boundary is compensated separately by one of the four terms in the diffraction coefficient, there is no problem in calculating the field when two boundaries are close to each other or in juxtaposition. This occurs when  $\phi' = 0$  or  $n\pi$  and when  $\phi'$  is close to  $n\pi/2$  with  $n \approx 1$ . The shadow and reflection boundaries are real if they occur in physical space, which is in the angular range from 0 to  $n\pi$ ; outside this range they are virtual boundaries. If a virtual boundary is close to the surface of the wedge, as it is when  $\phi'$  is close to  $\pi$  or  $(n-1)\pi$ , its transition region may extend into physical space near the wedge and significantly effect the calculation of the field there. The value of  $N^+$  or  $N^-$  at each boundary is included in Table 1 for convenience; as noted earlier, this is a stable quantity in the transition regions.

Next it will be shown that the product of the cotangents and the transition functions in Eq. (50) is finite, even at the shadow and reflection boundaries. To facilitate the discussion let

$$(58) \quad \beta = \phi \pm \phi' .$$

In the neighborhood of the shadow or reflection boundary

$$(59) \quad \beta = 2\pi nN^{\pm} \mp (\pi - \epsilon),$$

where  $\epsilon$  is positive in the region illuminated by the incident or reflected field. The  $\pm$  superscript of  $N$  is directly associated with the  $\mp$  sign in the equation above and the  $\pm$  sign in the argument of the cotangent below.

For  $\epsilon$  small,

$$(60) \cot\left(\frac{\pi \pm \beta}{2n}\right) \sim \frac{2n}{\epsilon},$$

and

$$(61) a^{\pm}(\beta) = 2 \cos^2\left(\frac{2\pi n N^{\pm} - \beta}{2}\right) \sim \frac{\epsilon^2}{2}.$$

The transition function  $F(X)$  is given by Eq. (51) with  $X = kLa^{\pm}(\beta)$ .

We are concerned with the case where  $kL$  is large but  $X$  is small, so that

$$(62) F(X) \sim \left( \sqrt{\pi X} - 2Xe^{j\frac{\pi}{4}} - \frac{2}{3}X^2 e^{-j\frac{\pi}{4}} \right) e^{j\left(\frac{\pi}{4} + X\right)}.$$

From Eqs. (60), (61) and (62),

$$(63) \cot\left(\frac{\pi \pm \beta}{2n}\right) F[kL a^{\pm}(\beta)] \simeq n \left( \sqrt{2\pi kL} \operatorname{sgn} \epsilon - 2kL\epsilon e^{j\frac{\pi}{4}} \right) e^{j\frac{\pi}{4}}$$

for  $\epsilon$  small. It is clear that the above expression is finite but discontinuous at the shadow and reflection boundaries. These discontinuities compensate the discontinuity in the incident or reflected field at these boundaries, as will be shown in the paragraphs to follow.

The high frequency approximation for the total field being considered here is the sum of the geometrical optics field and the asymptotic approximation of the diffracted field. It is convenient to give the components of these fields in the ray fixed coordinate system described on page 21; hence it will be necessary to transform

the components of the reflected field given in the first section to this coordinate system. We will begin by carrying out this transformation, which is facilitated by employing matrix notation.

From Eqs. (21) and (22) the reflected electric field

$$(64) \begin{bmatrix} E_{\parallel}^r \\ E_{\perp}^r \end{bmatrix} \sim \begin{bmatrix} 1 & 0 \\ 0 & -1 \end{bmatrix} \begin{bmatrix} E_{\parallel}^i \\ E_{\perp}^i \end{bmatrix} f(s),$$

where the subscripts  $\parallel$  and  $\perp$  denote components parallel and perpendicular to the ordinary plane of incidence and

$$(65) f(s) = \sqrt{\frac{\rho_1^i \rho_2^i}{(\rho_1^i + s)(\rho_2^i + s)}} e^{-jks}.$$

Note that for the plane surfaces forming the wedge,  $\rho_1^r = \rho_1^i$ ,  $\rho_2^r = \rho_2^i$ , where  $\rho_1^i$ ,  $\rho_2^i$  are the principal radii of curvature of the incident wavefront at the point of reflection. Equation (64) may be written more compactly as

$$(66) E^r \sim R E^i f(s).$$

The ordinary plane of incidence and the edge-fixed plane of incidence intersect along the incident ray passing through  $Q_E$ . The ordinary plane of incidence, the edge-fixed plane of reflection, and the cone of diffracted rays intersect at the ray reflected from  $Q_E$ . The edge-fixed plane of reflection contains the tangent to the edge and the ray reflected from  $Q_E$ . These planes and their lines of intersection are depicted in Fig. 9.

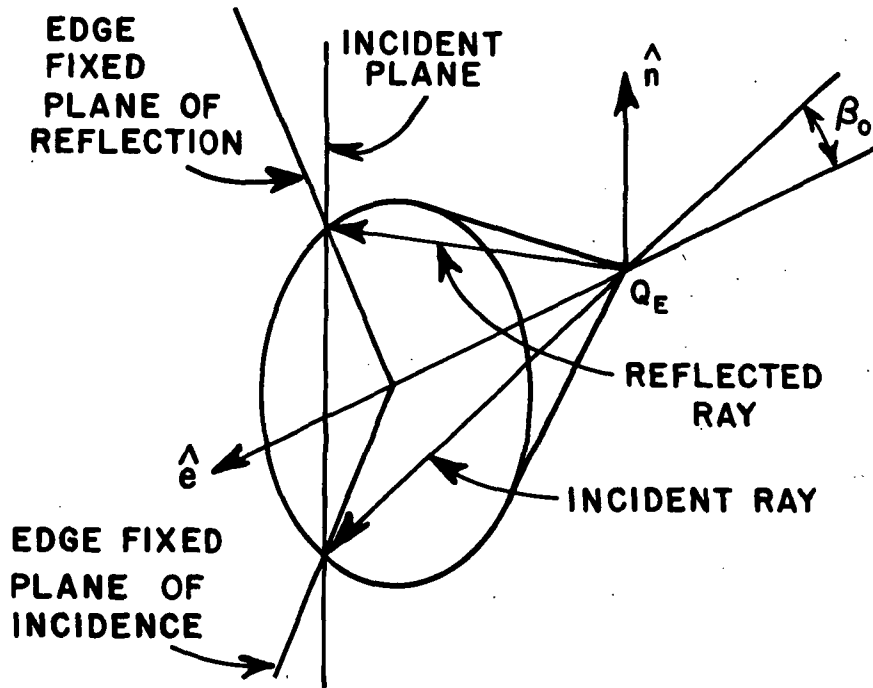


Fig. 9. Edge fixed plane of incidence and reflection.

Let the angle between the edge-fixed plane of incidence and the ordinary plane of incidence be  $-\alpha$ . In Appendix III it is shown that the angle between the edge-fixed plane of reflection and the ordinary plane of incidence is  $\alpha$ . The components of the incident electric field parallel and perpendicular to the edge-fixed plane of incidence are

$$(67a) \quad E_{\beta_0}^i = E_{\parallel}^i \cos \alpha - E_{\perp}^i \sin \alpha$$

$$(67b) \quad E_{\phi}^i = E_{\parallel}^i \sin \alpha + E_{\perp}^i \cos \alpha$$

or in the more compact matrix notation

$$(68) E^i' = T(-\alpha)E^i$$

where

$$(69) T(-\alpha) = \begin{bmatrix} \cos\alpha & -\sin\alpha \\ \sin\alpha & \cos\alpha \end{bmatrix}$$

From Eq. (66) the reflected electric field

$$(70) E^r \sim R E^i f(s) H(\epsilon)$$

in the neighborhood of the reflection boundary

$$(71) H(\epsilon) = \frac{1}{2} (1 + \operatorname{sgn} \epsilon)$$

is the unit step function.

The components of the reflected field parallel and perpendicular to the edge-fixed plane of reflection are given by

$$(72) T(\alpha)E^r = [T(\alpha)RT(-\alpha)^{-1}][T(-\alpha)E^i] f(s) H(\epsilon)$$

From Eq. (69) and R as given in Eq. (21),

$$(73) T(\alpha)R T(-\alpha)^{-1} = R;$$

hence from Eqs. (68), (70), (72) and (73)

$$(74) \quad \begin{bmatrix} E_{\beta_0}^r \\ E_{\phi}^r \end{bmatrix} \sim \frac{1}{2} \begin{bmatrix} 1 & 0 \\ 0 & -1 \end{bmatrix} \begin{bmatrix} E_{\beta_0}^i \\ E_{\phi}^i \end{bmatrix} f(s) (1 + \text{sgn } \epsilon).$$

The diffracted field close to the reflection boundary at  $\phi = \pi - \phi'$  is given by Eq. (31) together with Eqs. (50) and (63)

$$(75) \quad \begin{bmatrix} E_{\beta_0}^d \\ E_{\phi}^d \end{bmatrix} \sim \frac{-1}{2} \begin{bmatrix} 1 & 0 \\ 0 & -1 \end{bmatrix} \begin{bmatrix} E_{\beta_0}^i \\ E_{\phi}^i \end{bmatrix} \frac{\sqrt{L}}{\sin \beta_0} \sqrt{\frac{\rho_e^i}{s(\rho_e^i + s)}} e^{-jks} \text{sgn } \epsilon +$$

+ terms which are continuous at this boundary.

For the total field to be continuous at the reflection boundary, the sum of the discontinuous terms in Eqs. (74) and (75) must vanish; hence

$$(76) \quad -\frac{\sqrt{L}}{\sin \beta_0} \sqrt{\frac{\rho_e^i}{s(\rho_e^i + s)}} e^{-jks} + f(s) = 0,$$

so that the distance parameter

$$(77) \quad L = \frac{s(\rho_e^i + s) \rho_1^i \rho_2^i \sin^2 \beta_0}{\rho_e^i (\rho_1^i + s)(\rho_2^i + s)}$$

The behavior of the incident and diffracted fields at the shadow boundary  $\phi = \pi + \phi'$  may be treated in the same manner. After passing beyond  $Q_E$ , the electric field of the incident ray in the neighborhood of the shadow boundary is

$$(78) \quad \begin{bmatrix} E_{\beta_0}^i \\ E_{\phi}^i \end{bmatrix} \sim \frac{1}{2} \begin{bmatrix} -1 & 0 \\ 0 & -1 \end{bmatrix} \begin{bmatrix} E_{\beta_0}^i \\ E_{\phi}^i \end{bmatrix} f(s) (1 + \text{sgn } \epsilon).$$

The diffracted field close to this shadow boundary is

$$(79) \begin{bmatrix} E_{\beta_0}^d \\ E_{\phi}^d \end{bmatrix} \sim \frac{1}{2} \begin{bmatrix} 1 & 0 \\ 0 & 1 \end{bmatrix} \begin{bmatrix} E_{\beta_0}^i \\ E_{\phi}^i \end{bmatrix} \frac{\sqrt{L}}{\sin \beta_0} \sqrt{\frac{\rho_e^i}{s(\rho_e^i + s)}} e^{-jks} \operatorname{sgn} \epsilon +$$

+ in terms which are continuous at this shadow boundary.

For the total field to be continuous at the shadow boundary, the sum of the discontinuous terms in Eqs. (78) and (79) must vanish, and again it is seen that  $L$  is given by Eq. (77). Equation (77) is also obtained when the leading term in the high frequency approximation for the total field is made to be continuous at the other shadow and reflection boundaries. Also Eq. (77) reduces to Eq. (57) for the several types of incident waves for which formal asymptotic solutions were derived. We conclude therefore that the expression for  $L$  given by Eq. (77) is correct when the wedge is illuminated by an incident field with an arbitrary wavefront whose principal radii of curvature are  $\rho_1^i$  and  $\rho_2^i$ .

Since  $kL$  is the large parameter in the asymptotic approximation,  $\beta_0$  can not be arbitrarily small, which precludes grazing and near grazing incidence along the edge.

The commentary on Eq. (49) in the case of grazing incidence along the surface of the wedge also applies to Eq. (50), i.e., the diffraction coefficient  $D_h$  is multiplied by a factor of  $1/2$  and the diffraction coefficient  $D_s = 0$ .

If  $n = 1$  or  $2$ , it is apparent from Eq. (52) and the integral values of  $N^\pm$  that

$$(80) \quad a^\pm(\beta) = a(\beta) = 2 \cos^2 \frac{\beta}{2} .$$

Thus

$$\begin{aligned}
(81) \quad & \cot\left(\frac{\pi+\beta}{2n}\right) F[kLa^+(\beta)] + \cot\left(\frac{\pi-\beta}{2n}\right) F[kLa^-(\beta)] \\
&= \left[ \cot\left(\frac{\pi+\beta}{2n}\right) + \cot\left(\frac{\pi-\beta}{2n}\right) \right] F[kLa(\beta)] \\
&= \frac{-2 \sin \frac{\pi}{n}}{\cos \frac{\pi}{n} - \cos \frac{\beta}{n}} F[kLa(\beta)],
\end{aligned}$$

and from Eq. (50) the expressions for the scalar diffraction coefficients reduce to

$$(82) \quad D_{\frac{S}{h}}(\phi, \phi'; \beta_0) = \frac{e^{-j \frac{\pi}{4}} \sin \frac{\pi}{n}}{n \sqrt{2\pi k} \sin \beta_0} \left\{ \frac{F[kLa(\phi-\phi')]}{\cos \frac{\pi}{n} - \cos \frac{(\phi-\phi')}{n}} \mp \frac{F[kLa(\phi+\phi')]}{\cos \frac{\pi}{n} - \cos \frac{(\phi+\phi')}{n}} \right\}.$$

The edge vanishes for  $n = 1$  and the boundary surface is simply a perfectly-conducting plane of infinite extent. It is seen that the diffraction coefficients and diffracted field vanish for this case as expected.

If  $n = 2$  the wedge becomes a half plane and

$$(83) \quad D_{\frac{S}{h}}(\phi, \phi'; \beta_0) = \frac{-e^{-j \frac{\pi}{4}}}{2\sqrt{2\pi k} \sin \beta_0} \left\{ \frac{F[kLa(\phi-\phi')]}{\cos\left(\frac{\phi-\phi'}{2}\right)} \mp \frac{F[kLa(\phi+\phi')]}{\cos\left(\frac{\phi+\phi'}{2}\right)} \right\}$$

which can be written in the form

$$(84) D_{\frac{S}{h}}(\phi, \phi'; \beta_0) =$$

$$\frac{-e^{-j\frac{\pi}{4}}}{\sin \beta_0} \sqrt{\frac{L}{\pi}} \left[ f(kL, \phi - \phi') e^{j2kL \cos^2\left(\frac{\phi - \phi'}{2}\right) \operatorname{sgn}(\pi + \phi' - \phi)} \mp \right. \\ \left. \mp f(kL, \phi + \phi') e^{j2kL \cos^2\left(\frac{\phi + \phi'}{2}\right) \operatorname{sgn}(\pi - \phi' - \phi)} \right],$$

where

$$(85) f(kL, \beta) = \int_0^{\infty} \frac{e^{-j\tau^2}}{\sqrt{2kL} |\cos \frac{\beta}{2}|} d\tau,$$

a Fresnel integral.

When the diffraction coefficients given by Eq. (84) are used to calculate the fields diffracted by hard or soft half planes illuminated by a plane wave,  $L = s \sin^2 \beta_0$  and the result is in agreement with a solution obtained by Sommerfeld[9,24]. Since Sommerfeld's solution is an exact solution, we know that our solution is exact for this case too. If these half planes are illuminated by a cylindrical wave whose radius of curvature is  $r'$ ,  $L = rr'/(r+r')$  in which  $r$  is the perpendicular distance from the field point to the edge, and our solution reduces to an approximate solution deduced by Rudduck[25] from the work of Obha[26] and Nomura[27]. Rudduck and his coworkers have applied this solution to a number of two-dimensional antenna and scattering problems with good accuracy.

In this section on diffraction by wedges, diffraction coefficients have been obtained which may be used at all aspects surrounding the wedge, including the transition regions adjacent to shadow and reflection boundaries. The diffraction by curved edges in plane surfaces and curved sheets will be considered in the next section.

### B. The Curved Edge

The diffraction by curved edges will be treated in this section. As in the preceding section our solution is based on Keller's method of the canonical problem. The justification of the method is that high-frequency diffraction like high-frequency reflection is a local phenomenon, and locally one can approximate the curved edge geometry by a wedge, where the straight edge of the wedge is tangent to the curved edge at the point of incidence  $Q_E$  in Figs. 5a,b, and its plane surfaces are tangent to the surfaces forming the curved edge. The reflection coefficient for the curved surface derived in Section I could have been found by this method, choosing the reflection of plane waves at a plane surface as the canonical problem. With these assumptions, the results of the preceding section can be applied directly to the curved edge problem. As we have just noted, there is an equivalent wedge (with exterior wedge angle  $n\pi$ ) associated with every curved edge structure, and so in generalizing the solution for the wedge, it is only necessary to modify the expressions for the distance parameter  $L$ , which appear in the arguments of the transition functions.

In the present treatment we do not show that our solution can be matched to a boundary layer solution valid at and near the curved edge.

It would be desirable to carry this out to confirm the validity of our solution and possibly to obtain additional terms in the asymptotic approximation. Ahluwalia<sup>13</sup> has used a boundary layer solution in this way to obtain an asymptotic expansion for the scalar field diffracted by a curved edge; however his representation of the total field differs from the one given here. It does not appear as separate contributions from the incident, reflected and diffracted fields.

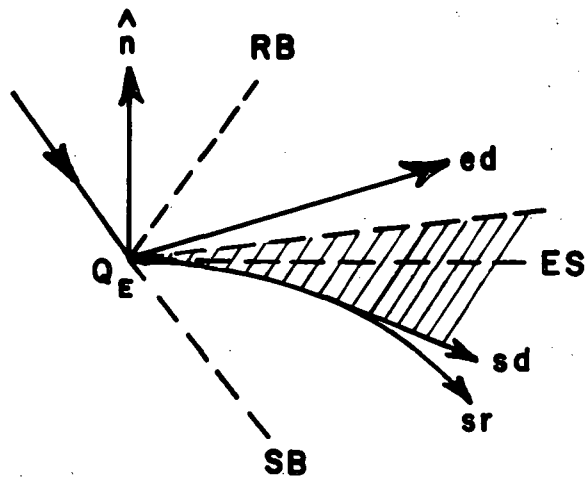
The diffraction by a curved edge in a plane screen affords the simplest example of curved edge diffraction. The scalar diffraction coefficients appearing in Eq. (45) are given by Eqs. (83) or (84), and since  $\rho = \rho_e^i$  on both the shadow and reflection boundaries,  $L$  is the distance parameter given by Eq. (77). At aspects other than incidence and reflection,  $\rho$  within the square root term of Eq. (31) must be found from Eq. (32). As in the case of the wedge, we obtain a high-frequency approximation at all points surrounding the edge, which are not too close to the edge or to caustics of the diffracted field.

The diffraction by a curved edge in a curved screen ( $n=2$ ) is next in the order of increasing difficulty. Whenever the surface forming the edge is curved, the region near it is dominated by surface diffraction phenomena, which is particularly important on the convex side. On the convex side of the curved screen there are surface ray modes, also known as creeping waves, which shed energy tangentially as they propagate along the surface. As a result of this, the radiation leakage phenomenon is significant in a considerable region

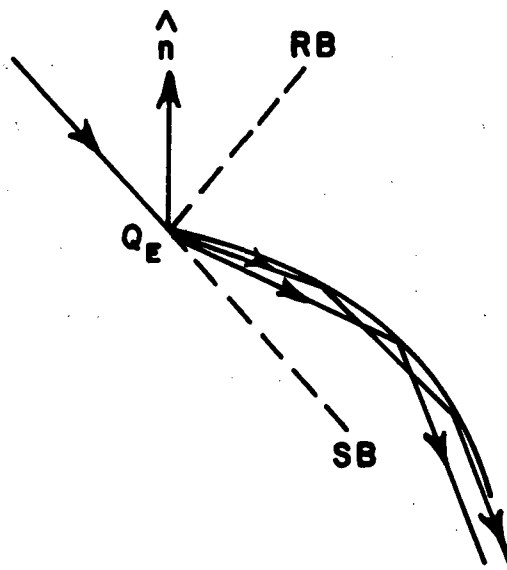
near the surface. On the concave side of the curved screen we have bound modes that do not leak energy as they propagate; these modes are known as whispering gallery modes. Both types of modes are excited by an illuminated edge in a curved surface; however they also may be excited by the incident field. As mentioned earlier, surface diffraction phenomena have been neglected in the present treatment; hence the region between the convex surface and the boundary ES between the edge diffracted and surface diffracted rays must be excluded. The boundary ES is formed by the intersection of the cone of diffracted rays and the plane tangent to the surface at  $Q_E$ ; in general it does not lie in the ordinary plane of incidence. In addition, the transition region adjacent to the boundary must be excluded. This region from which the field and source points are to be excluded appears as the shaded portion of Fig. 10a, where all rays and boundaries are shown projected on the plane perpendicular to the edge at  $Q_E$ . It should be noted that in general the projection of the surface ray  $S_r$  does not coincide with the intersection of the boundary surface S and the plane of projection.

On the concave side the whispering gallery effect can be described approximately by geometrical optics in the form of a series of reflected waves whose rays form cords along the concave reflecting surface as indicated in Fig. 10b. As glancing incidence is approached, the cord length diminishes and the description of the phenomenon in terms of a sequence of reflections breaks down; the geometrical optics analysis must be truncated at this point. If the errors resulting

from this truncation are not serious, the radiation from the concave side can be included in the present analysis.



(a) CONVEX SIDE



(b) CONCAVE SIDE

Fig. 10. Diffraction at the edge of a curved screen.

In this case  $n = 2$ , and the scalar diffraction coefficients in Eq. (45) are given by

$$(86) D_{\frac{h}{h}}(\phi, \phi'; \beta_0) =$$

$$\frac{-e^{-j \frac{\pi}{4}}}{2\sqrt{2\pi k} \sin \beta_0} \left\{ \frac{F[kL^i a(\phi - \phi')]}{\cos\left(\frac{\phi - \phi'}{2}\right)} \mp \frac{F[kL^r a(\phi + \phi')]}{\cos\left(\frac{\phi + \phi'}{2}\right)} \right\}$$

in which the first term is discontinuous at the shadow boundary, whereas the second is discontinuous at the reflection boundary. Unlike the reflection from a plane surface, the divergence or spreading of the wave reflected from a curved surface is different from that of the incidence wave; hence the radii of curvature of the reflected and diffracted wavefronts at the shadow boundary are distinct from the radii of curvature of the incident and diffracted wavefronts at the shadow boundary.

Employing arguments similar to those used to find the distance parameter for the wedge

$$(87a) \quad L^i = \frac{s(\rho_e^i + s) \rho_1^i \rho_2^i \sin^2 \beta_0}{\rho_e^i (\rho_1^i + s)(\rho_2^i + s)},$$

$$(87b) \quad L^r = \frac{s(\rho_e^r + s) \rho_1^r \rho_2^r \sin^2 \beta_0}{\rho_e^r (\rho_1^r + s)(\rho_2^r + s)},$$

where  $\rho_e^i$ ,  $\rho_1^i$ ,  $\rho_2^i$  are defined as before,  $\rho_1^r$  and  $\rho_2^r$  are the principal radii of curvature of the reflected wavefront at  $Q_E$ , and from Eq. (32)

$$(88) \quad \frac{1}{\rho_e^r} = \frac{1}{\rho_e^i} - \frac{2(\hat{n} \cdot \hat{n}_e)(\hat{s}^i \cdot \hat{n})}{a \sin^2 \beta_0}$$

As  $\phi'$  approaches  $\pi$  we approach grazing incidence as shown in Fig. 11. Then since  $\rho_1^r \rho_2^r \rightarrow 0$ ,  $L^r \rightarrow 0$  and Eq. (86) can no longer be used to calculate the scalar diffraction coefficients. Under these circumstances the shadow and reflection boundaries usually lie within the shaded region in Fig. 11, and the transition regions associated with edge diffraction overlap those associated with surface diffraction. If the field and source points are both sufficiently far from the edge, we may set the transition functions in Eq. (86) equal to unity. On the otherhand, for the field point or source point close to the edge or for both points close to the edge, we may be able to use reciprocity (see Appendix IV) to calculate the field at P in Fig. 11, if the distance parameters for a unit source located at P are large enough.

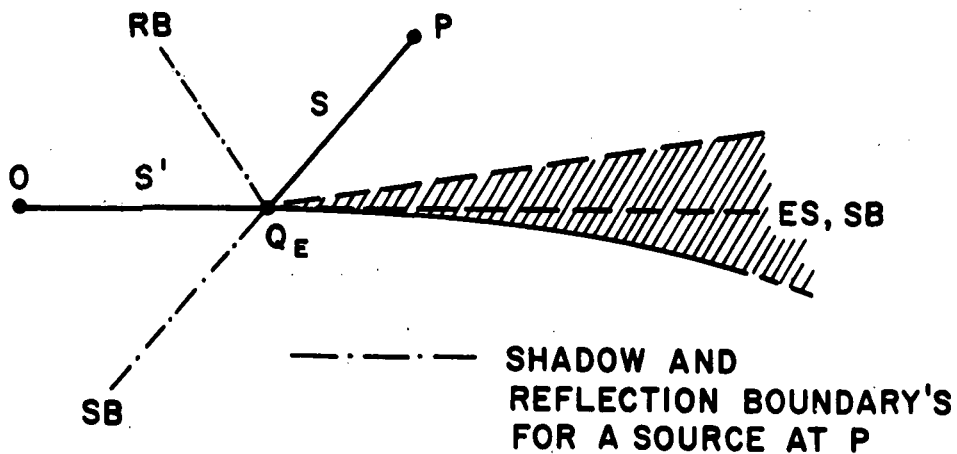


Fig. 11. Grazing incidence on the edge of a curved screen.

We conclude this chapter by finding the scalar diffraction coefficients for a curved edge in an otherwise smooth curved surface. Again we seek diffraction coefficients which can be used in the transition regions associated with the shadow and reflection boundaries of this structure. Both surfaces forming the curved edge may be convex, both surfaces may be concave, one surface may be convex and the other concave, or one surface may be plane and the other convex or concave.

First let us consider the simple case which occurs when the illuminated surface forming the curved edge is plane, as it may be at the base of a cylinder or cone. For this configuration the reflected field is found directly from the incident field, as it is in the case of the wedge, e.g., it may be easily deduced from image theory. Thus the scalar diffraction coefficients are found directly from Eq. (50) and the distance parameter from Eq. (77). The calculated diffracted field may not be accurate close to the shadowed surface if surface diffraction phenomena are significant.

The more general problem where the illuminated surface is curved is closely related to the diffraction by a curved edge in a curved screen which has just been discussed; for example, the field point and source point must not be too close to a convex surface and the case of grazing incidence must be treated separately.

We introduce the wedge tangent to the boundary surfaces of the curved edge at  $Q_E$ . The boundary ES is formed by the intersection of this wedge with the cone of diffracted rays. Away from the boundary ES on the cone of diffracted rays the scalar diffraction coefficients are given by Eq. (50), except that distance parameter  $L$  in the argument of

each of the four transition functions may be different. As before  $L$  is found in each case by requiring the total field to be continuous at each shadow and reflection boundary.

It is seen from Figs. 7a,b that  $N^+$ ,  $N^-$  associated with the shadow boundaries at  $\phi' - \pi$ ,  $\phi' + \pi$  are different from zero only at angular distances greater than  $\pi$  from these boundaries. When this angular distance exceeds  $\pi$  the field point is usually outside the transition region in question, unless  $kL$  is small. In view of the assumptions involved in extending the wedge solution to the curved edge, the validity of the approximation is in question for such small values of  $kL$ , so they are excluded here. These considerations and analogous considerations lead us to set the  $N^\pm$  equal to the values they have in Table I.

Then

$$(89) \quad D_{\frac{S}{h}}(\phi, \phi'; \beta_0) = \frac{e^{-j \frac{\pi}{4}}}{2n \sqrt{2\pi k} \sin \beta_0} \times \left[ \frac{2 \sin \frac{\pi}{n} F[kL^i a(\phi - \phi')]}{\cos \frac{\pi}{n} - \cos\left(\frac{\phi - \phi'}{n}\right)} \pm \left\{ \cot\left(\frac{\pi + (\phi + \phi')}{2n}\right) F[kL^{rn} a^+(\phi + \phi')] + \cot\left(\frac{\pi - (\phi + \phi')}{2n}\right) F[kL^{ro} a(\phi + \phi')] \right\} \right],$$

in which  $a(\beta) = 2 \cos^2 \frac{\beta}{2}$

and  $a^+(\beta) = 2 \cos^2 \frac{2\pi n - \beta}{2}$

Again employing arguments similar to those used to find the distance parameters for the edge, one finds that  $L^i$  is given by Eq. (87a), and that  $L^{ro}$ ,  $L^{rn}$  are given by Eq. (87). The additional superscripts  $o$  and  $n$  denote that the radii of curvature are calculated at the reflection boundaries  $\pi - \phi'$  and  $(2n-1)\pi - \phi'$ , respectively.

Although the reasoning employed to find the distance parameters is the same as that used in the preceding cases, namely that the total field be continuous at the shadow and reflection boundaries, a problem arises which was not encountered earlier. For a given aspect of incidence it is clear that only two of the boundaries associated with the three transition functions exist, the other boundary is outside real space. Since neither the field or source points are permitted close to grazing incidence at  $\phi' = 0$  or  $n\pi$ , it is reasonable to set the transition function, which is associated with the boundary located outside the interval  $0 < \phi < n\pi$ , equal to one.

At grazing incidence  $\phi' = \pi$  or  $(n-1)\pi$  for which  $L^{r0}$  or  $L^{rn}$  vanish, the scalar diffraction coefficients are calculated by the same procedure used for the curved screen at grazing incidence  $\phi' = \pi$ .

In the far zone where  $s \gg$  the principal radii of curvature  $\rho_1, \rho_2$  of the incident and reflected wavefronts at  $Q_E$  and the radius of curvature  $\rho$  of the diffracted wavefront at  $Q_E$  in the directions of incidence and reflection, Eqs. (77), (87a), and (87b) simplify to the form

$$(90) \quad L = \frac{\rho_1 \rho_2 \sin^2 \beta_0}{\rho_e} ;$$

the appropriate superscripts are omitted here for the sake of notational simplicity.

An interesting case occurs if there is a caustic of the incident, reflected or diffracted wave on a shadow or reflection boundary. The radii of curvature  $\rho_1, \rho_2$  or  $\rho$  associated with such a caustic are negative, and  $L$  may be either negative or positive. If  $L$  is positive, the presence of caustics at these boundaries presents no difficulty, except at points near

the caustic itself. On the otherhand if  $L$  is negative, there is a problem because the transition function has two branches each with an imaginary argument. We will restrict our attention to the situation where all the caustics on the boundary lie between the field point and the edge; this may occur in far-zone field calculations for example.

As pointed out in the last paragraph of Appendix II, if  $L$  is negative the incident (or reflected) field has one more caustic on the shadow (or reflection) boundary than does the diffracted field. This means that the phase of the transition function must change by an additional  $\pi/2$  as one moves from a point outside the transition region to the boundary, so that the transition function must have a total phase variation of  $3\pi/4$  instead of the  $\pi/4$  phase variation shown in Fig. 6. An examination of the two branches of the transition function at the boundary and outside the transition region reveals that they do not have the proper behavior.

When a curved strip is illuminated by a plane wave from its concave side, there is a caustic of the reflected field on the reflection boundaries. In treating the scattering from this strip we have found that an adequate function is provided by

$$|F(k|L|a)|e^{j3[\text{phase of } F(k|L|a)]}$$

in which  $F(k|L|a)$  is the ordinary transition function given by Eq. (51). (Note that  $L$  and  $a$  may have superscripts). In spite of the fact that the above expression has the proper behavior outside transition regions and at shadow or reflection boundaries and also appears to yield good numerical results, it lacks theoretical justification. A satisfactory derivation of the transition function for  $L$  negative is being sought.

#### IV. DISCUSSION

A dyadic diffraction coefficient has been obtained for an electromagnetic wave obliquely incident on a curved edge formed by perfectly-conducting curved or plane surfaces. Unlike the edge diffraction coefficient of Keller's original theory, this diffraction coefficient is valid in the transition regions of the shadow and reflection boundaries. Although the diffraction coefficient has been given in dyadic form in the earlier chapters, it can also be represented in matrix form, so that the high-frequency diffracted electric field can be written

$$(91) \quad \begin{bmatrix} E_{\beta_0}^d \\ E_{\phi}^d \end{bmatrix} = \begin{bmatrix} -D_s & 0 \\ 0 & -D_h \end{bmatrix} \begin{bmatrix} E_{\beta_0}^i \\ E_{\phi}^i \end{bmatrix} \sqrt{\frac{\rho}{s(\rho+s)}} e^{-jks},$$

and since the high-frequency diffracted magnetic field

$$(92) \quad \vec{H}^d = Y_c \hat{s} \times \vec{E}^d,$$

$$(93) \quad \begin{bmatrix} H_{\phi}^d \\ H_{\beta_0}^d \end{bmatrix} = \begin{bmatrix} -D_s & 0 \\ 0 & -D_h \end{bmatrix} \begin{bmatrix} H_{\phi}^i \\ H_{\beta_0}^i \end{bmatrix} \sqrt{\frac{\rho}{s(\rho+s)}} e^{-jks}$$

in which  $D_s$ ,  $D_h$  are given by

- (a) Eq. (89) for the curved edge (general case),
  - (b) Eq. (86) for a curved edge in a curved screen,
  - (c) Eq. (83) or (84) for a curved or straight edge in a plane screen,
- and  $\rho$  is given by Eq. (32).

(d) Eq. (50) for the wedge,

It is pointed out in Section IIIB that the scalar diffraction coefficients in cases (a) and (b) are not valid at aspects of incidence and diffraction close to grazing on a convex surface forming the edge at the point of diffraction. Work is in progress to remove this limitation. Also grazing incidence on a plane surface is a special case which requires the introduction of a factor of  $1/2$  when calculating the diffracted field, see the discussion of page 27.

The large parameters are  $kL$  or  $kL^i$ ,  $kL^r$  in the asymptotic approximation; hence when these are small our GTD representation of the diffracted field is no longer valid. Thus source or field points close to the edge ( $s$  or  $s'$  small) must be excluded; also aspects of incidence close to edge-on incidence ( $\beta_0$  small) must be excluded. Edge-on incidence is a separate phenomenon, which has been discussed by Ryan and Peters [28] and by Senior [29].

Outside of the transition regions where the arguments of the transition functions are greater than 10, the expressions for the scalar diffraction coefficients all simplify to Eq. (49). Usually the field point is only in one transition region at a time, so that the calculation of the diffracted field is simplified because only one of the transition functions is significantly different from unity.

One would expect the diffraction coefficients for the wedge to be more accurate than those for the curved edge, because the canonical problems involve wedge diffraction. If the curved edge

were used as a canonical problem, one would anticipate the presence of additional terms in the asymptotic solution for the diffracted field; these terms would depend upon the radius of curvature of the edge at the point of diffraction and its derivatives with respect to distance along the edge. This is verified by the work of Buchal and Keller [30] and Wolfe [31], who treated the diffraction of a scalar plane wave normally incident on a plane screen with a curved edge.

In calculating the diffracted field, it is assumed that the incident field is slowly varying at the point of diffraction, except for its phase variation along the incident ray. If the incident field is rapidly varying at the point of diffraction, it is usually possible to express it as a sum of slowly-varying component fields, so that the diffracted field of each component can be calculated in the usual way and the total diffracted field obtained by superposition. Alternatively, in calculating the diffracted field, one could introduce higher order terms which depend upon the spatial derivatives of the incident field at the point of diffraction. Expressions of this type were obtained by Zitron and Karp [32] in their treatment of the scattering from cylinders; they are also derived in reference 11.

In the text it is pointed out that Eqs. (91) and (93) can not be used to calculate the field at a caustic of the diffracted ray. At such a caustic it is convenient to use a supplementary solution in the form of an integral representation of the field. The equivalent sources in this representation are determined from a suitable high-frequency approximation, such as geometrical optics or the GTD. In

the case of an axial caustic, it is convenient to employ equivalent electric and magnetic edge currents introduced by Ryan and Peters [33]; the use of these edge currents is also described in Reference [34].

In conclusion we note that the geometrical optics field and our expression for the edge-diffracted field are both asymptotic solutions of Maxwell's equations. The total high-frequency field is the sum of these two fields, and away from the edge it is everywhere continuous, except at caustics. Our solution reduces to known asymptotic solutions for the wedge, and it has been found to yield the first two or three terms in the asymptotic expansion of the diffracted fields of problems which can be solved differently. Furthermore, the numerical results obtained by its application to a number of examples are found to be in excellent agreement with rigorously-calculated and measured values. Also we have been able to show that our solution is consistent with the reciprocity principle, see Appendix IV.

APPENDIX I  
THE CAUSTIC DISTANCE FOR REFLECTION

The principal radii of curvature of the reflected wavefront  $\rho_1^r, \rho_2^r$  and the principal directions (axes) of the wavefront will be determined in this appendix. The plane of incidence may be different from the principal planes of the reflecting surface, so that the principal directions of the incident wavefront are quite distinct from those of the reflecting surface.

This problem has been treated both by Fock [35] and by Deschamps; [36] however they did not find the principal radii of curvature nor the principal directions of the reflected wavefront. Fock used a surface-fixed coordinate system to formulate his solution, and he evaluated the resulting 3 x 3 determinant for the divergence factor  $D(S)$  of the reflected wave after some rather complicated tensor analysis. On the otherhand, Deschamps formulated his solution in a ray-fixed coordinate system,\* and employing elementary matrix theory together with straightforward coordinate transformations, he obtained a 2 x 2 curvature matrix for the reflected wave from that of the incident wave. We will find  $\rho_1^r, \rho_2^r$  and their principal directions by diagonalizing his curvature matrix.

Let us begin by defining the curvature matrix employed by Deschamps. Consider the curved surface

---

\*The advantages inherent in using ray-fixed coordinate systems in treating ray optical problems have already been noted in the text.

$$(A-1) \quad z = f(x,y)$$

with the z axis normal to the surface at the point P where  $x,y,z = 0$ .

Thus

$$(A-2) \quad f_x = f_y = 0$$

where

$$f_x = \frac{\partial f}{\partial x}, \quad f_{xx} = \frac{\partial^2 f}{\partial x^2}, \text{ etc.}$$

are evaluated at  $x,y = 0$ .

In the neighborhood of the origin

$$(A-3) \quad z = \frac{1}{2} [f_{xx} x^2 + 2f_{xy} xy + f_{yy} y^2]$$

$$= \frac{1}{2} \left[ \frac{x^2}{\rho_1} + \frac{y^2}{\rho_2} \right]$$

in which  $\rho_1, \rho_2$  are the principal radii of curvature in the principal directions  $\hat{X}, \hat{Y}$  respectively. With

$$\bar{x} = x \hat{x} + y \hat{y} \quad \text{and} \quad \bar{X} = X \hat{X} + Y \hat{Y}$$

Eq. (A-3) may be written in matrix notation

$$(A-4) \quad z = \frac{1}{2} x Q x = \frac{1}{2} X Q_0 X,$$

in which Q is a 2 x 2 symmetric matrix and  $Q_0$  is its diagonal form.

The matrices Q and  $Q_0$  are referred to as curvature matrices

$$(A-5) \quad Q = \begin{bmatrix} f_{xx} & f_{xy} \\ f_{xy} & f_{yy} \end{bmatrix},$$

and

$$(A-6) \quad Q_0 = \begin{bmatrix} \frac{1}{\rho_1} & 0 \\ 0 & \frac{1}{\rho_2} \end{bmatrix}.$$

The Gaussian curvature of the surface

$$(A-7) \quad K = \text{determinant of } Q \equiv |Q| = |Q_0|.$$

Let a wavefront be incident on a curved surface  $S$  at  $Q_R$  as shown in Fig. 2A.

$\hat{U}_1, \hat{U}_2$  are unit vectors in the principal directions of  $S$  at  $Q_R$  with principal radii of curvature  $R_1, R_2$ .

$\hat{X}_1^i, \hat{X}_2^i$  are the principal directions of the incident wavefront at  $Q_R$  with principal radii of curvature  $\rho_1^i, \rho_2^i$ .

$\hat{x}_1^r, \hat{x}_2^r$  are unit vectors perpendicular to the reflected ray; they are determined by reflecting the unit vectors  $\hat{X}_1^i, \hat{X}_2^i$  in the plane tangent to  $S$  at  $Q_R$ , i.e.,

$$(A-8) \quad \hat{x}_1^r = \hat{X}_1^i - 2(\hat{n} \cdot \hat{X}_1^i)\hat{n},$$

see Fig. 2A. As will be seen,  $\hat{x}_1^r, \hat{x}_2^r$  are not in the principal directions of the reflected wavefront. We now define

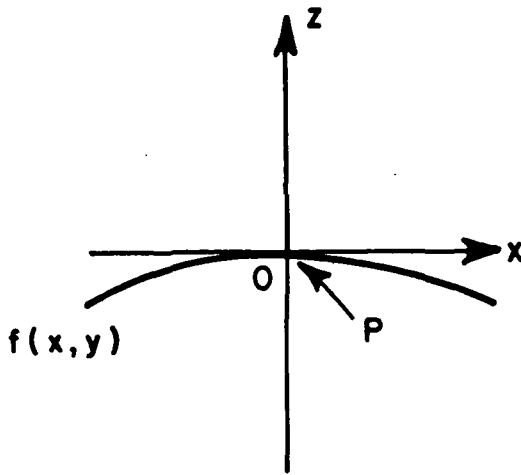


Fig. 1A. A smooth curved surface near the point P.

$$(A-9) \quad Q_0^i = \begin{bmatrix} \frac{1}{\rho_1} & 0 \\ 0 & \frac{1}{\rho_2} \end{bmatrix},$$

$$(A-10) \quad C_0 = \begin{bmatrix} \frac{1}{R_1} & 0 \\ 0 & \frac{1}{R_2} \end{bmatrix},$$

and

$$(A-11) \quad \theta = \begin{bmatrix} \hat{x}_1^i \cdot \hat{u}_1 & \hat{x}_1^i \cdot \hat{u}_2 \\ \hat{x}_2^i \cdot \hat{u}_1 & \hat{x}_2^i \cdot \hat{u}_2 \end{bmatrix}$$

Deschamps has shown that the curvature matrix for the reflected wavefront

$$(A-12) \quad Q^r = Q_0^i - 2(\theta^{-1})^T C_0 \theta^{-1} \cos \theta^i$$

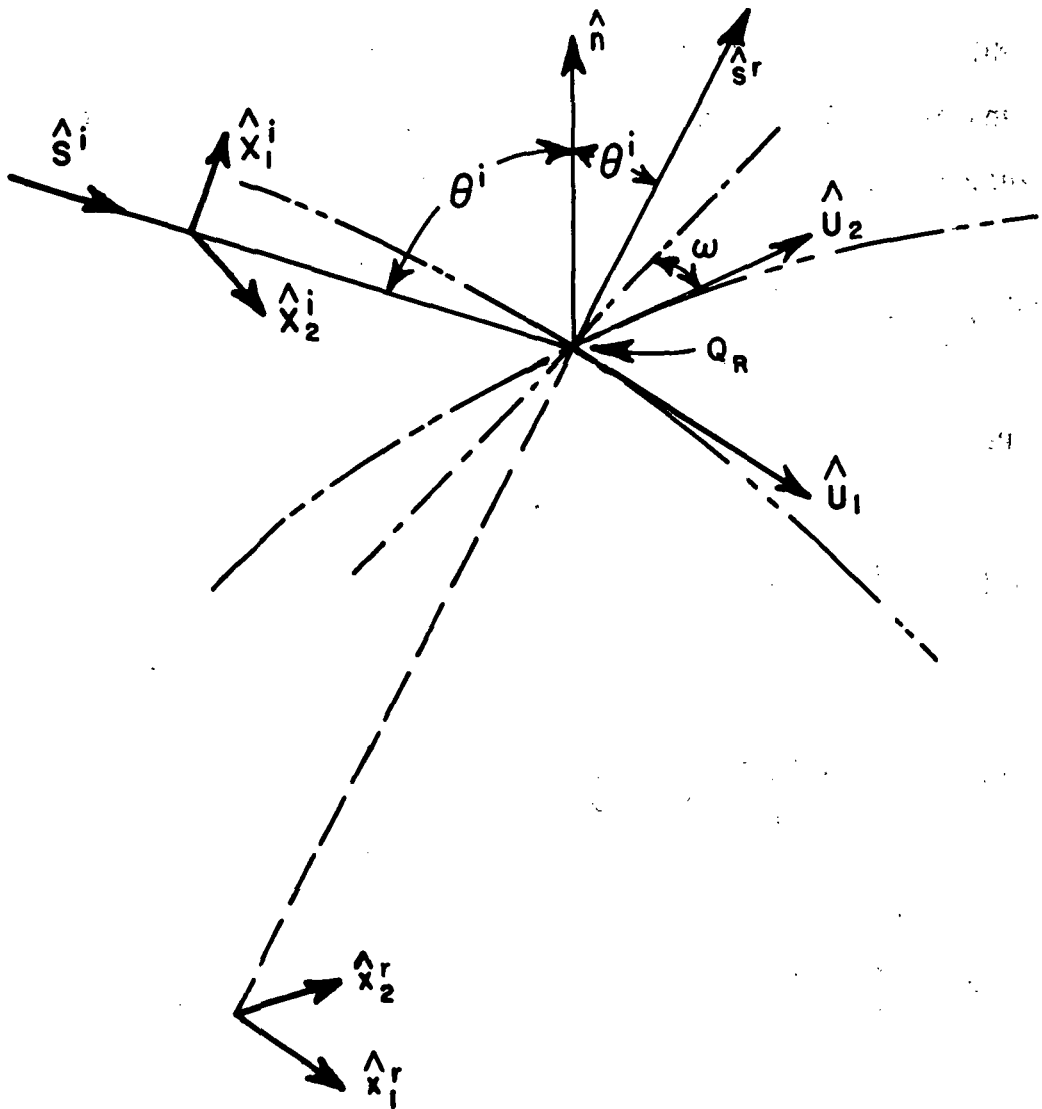


Fig. 2A. Geometry for the analysis of the reflected wavefront. The reflecting surface is S.

- Intersection of a principal plane of S at  $Q_R$  with S
- Intersection of the plane of incidence with the plane tangent to S at  $Q_R$
- Extension of the reflected ray below S.

in which the superscript -1 denotes the inverse matrix, the superscript T denotes the transpose matrix and  $\theta^i$  is the angle of incidence as before. A result equivalent to Eq. (12) has been obtained by Fock.

$$(A-13) \quad Q^r = \begin{bmatrix} Q_{11}^r & Q_{12}^r \\ Q_{12}^r & Q_{22}^r \end{bmatrix}$$

where

$$(A-14a) \quad Q_{11}^r = \frac{1}{\rho_1^i} - \frac{2 \cos \theta^i}{|\theta|^2} \left[ \frac{(\theta_{22})^2}{R_1} + \frac{(\theta_{21})^2}{R_2} \right]$$

$$(A-14b) \quad Q_{12}^r = \frac{2 \cos \theta^i}{|\theta|^2} \left[ \frac{\theta_{22}\theta_{12}}{R_1} + \frac{\theta_{11}\theta_{22}}{R_2} \right]$$

$$(A-14c) \quad Q_{22}^r = \frac{1}{\rho_2^i} - \frac{2 \cos \theta^i}{|\theta|^2} \left[ \frac{(\theta_{12})^2}{R_1} + \frac{(\theta_{11})^2}{R_2} \right]$$

with

$$(A-14d) \quad \theta_{jk} = \hat{X}_j^i \cdot \hat{U}_k$$

We have diagonalized  $Q^r$  to find its eigenvalues  $1/\rho_1^r, 1/\rho_2^r$ .

$$\begin{aligned}
\text{(A-15)} \quad \frac{1}{r_{\rho_1^r}} &= \frac{1}{2} \left( \frac{1}{\rho_1^i} + \frac{1}{\rho_2^i} \right) + \frac{\cos \theta^i}{|\theta|^2} \left[ \frac{(\theta_{22})^2 + (\theta_{12})^2}{R_1} + \frac{(\theta_{21})^2 + (\theta_{11})^2}{R_2} \right] \\
&\pm \frac{1}{2} \sqrt{\left( \frac{1}{\rho_1^i} - \frac{1}{\rho_2^i} \right)^2 + \left( \frac{1}{\rho_1^i} - \frac{1}{\rho_2^i} \right) \frac{4 \cos \theta^i}{|\theta|^2} \left[ \frac{(\theta_{22})^2 - (\theta_{12})^2}{R_1} + \frac{(\theta_{21})^2 - (\theta_{11})^2}{R_2} \right] +} \\
&+ \frac{4 \cos \theta^i}{|\theta|^2} \left[ \left( \frac{(\theta_{22})^2 + (\theta_{12})^2}{R_1} + \frac{(\theta_{21})^2 + (\theta_{11})^2}{R_2} \right)^2 - \frac{4 |\theta|^2}{R_1 R_2} \right]}
\end{aligned}$$

in which the + sign associated with  $\rho_1^r$  and the - sign with  $\rho_2^r$ . As noted in the discussion following Eqs. (23a,b) in the text, this equation has the form of an elementary mirror formula, except that the reciprocal of the object distance is replaced by the mean curvature of the incident wavefront.

The incident spherical wavefront is frequently of interest; let us simplify Eq. (A-15) for this case. For the spherical wave  $\hat{\chi}_1^i, \hat{\chi}_2^i$  can be chosen in any way convenient. Let  $\hat{\chi}_1^i$  be in the plane of incidence;  $\hat{\chi}_2^i$  is then parallel to the plane tangent to the surface of reflection at  $Q_R$ . Referring to Fig. 2A,

$$\text{(A-16a)} \quad \hat{\chi}_1^i = -\cos \theta^i \sin \omega \hat{U}_1 + \cos \theta^i \cos \omega \hat{U}_2 + \sin \theta^i \hat{n},$$

$$\text{(A-16b)} \quad \hat{\chi}_2^i = \cos \omega \hat{U}_1 + \sin \omega \hat{U}_2,$$

where  $\omega$  is the angle between the plane of incidence and the  $\hat{n}, \hat{u}_2$  principal plane of the reflecting surface.

$$(A-17a) \quad \theta_{11} = -\cos \theta^i \sin \omega$$

$$(A-17b) \quad \theta_{12} = \cos \theta^i \cos \omega$$

$$(A-17c) \quad \theta_{21} = \cos \omega$$

$$(A-17d) \quad \theta_{22} = \sin \omega$$

Using the above Eqs.

$$(A-18) \quad |\theta| = -\cos \theta^i;$$

furthermore

$$(A-19a) \quad \frac{1}{2} \left( \frac{1}{\rho_1} + \frac{1}{\rho_2} \right) = \frac{1}{s^T}$$

$$(A-19b) \quad \left( \frac{1}{\rho_1} - \frac{1}{\rho_2} \right) = 0.$$

Hence, substituting Eqs. (A-17), (A-18) and (A-19) into Eq. (A-15),

$$(A-20) \quad \frac{1}{\rho_1^r} = \frac{1}{s^r} + \frac{1}{\cos \theta^i} \left[ \frac{\sin^2 \theta_2}{R_1} + \frac{\sin^2 \theta_1}{R_2} \right] \pm \frac{1}{\cos^2 \theta^i} \left[ \frac{\sin^2 \theta_2}{R_1} + \frac{\sin^2 \theta_1}{R_2} \right]^2 - \frac{4}{R_1 R_2}$$

with

$$(A-21a) \quad \sin^2 \theta_1 = \cos^2 \omega + \sin^2 \omega \cos^2 \theta^i,$$

$$(A-21b) \quad \sin^2 \theta_2 = \sin^2 \omega + \cos^2 \omega \cos^2 \theta^i.$$

$\theta_1$  is the angle between the direction of the incident ray  $\hat{s}^i$  and  $\hat{U}_1$ , whereas  $\theta_2$  is the angle between  $\hat{s}^i$  and  $\hat{U}_2$ . Equation (A-20) was obtained by Kouyoumjian several years earlier using a different method.

We conclude this section by giving the eigenvectors of  $Q_r$ ; these yield the principal directions of the reflected wavefront with respect to the  $x_1^r, x_2^r$  coordinates.

$$(A-22) \quad \hat{x}_1^r = \frac{\left[ \left( Q_{22} - \frac{1}{r} \right) \hat{x}_1^r - Q_{12} \hat{x}_2^r \right]}{\sqrt{\left( Q_{22} - \frac{1}{r} \right)^2 + Q_{12}^2}}$$

$$(A-23) \quad \hat{x}_2^r = -\hat{s}^r \times \hat{x}_1^r .$$

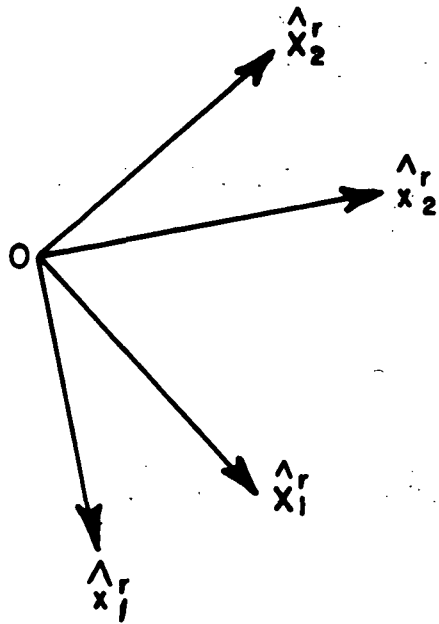


Fig. 3A. Principal directions of the reflected wavefront with respect to the  $x_1^r, x_2^r$  coordinates.

It should be noted that the principal directions of the wavefront are distinct from the principal directions associated with the reflection matrix; as pointed out in the text the latter are parallel and perpendicular to the plane of incidence.

APPENDIX II  
THE EDGE CAUSTIC DISTANCE

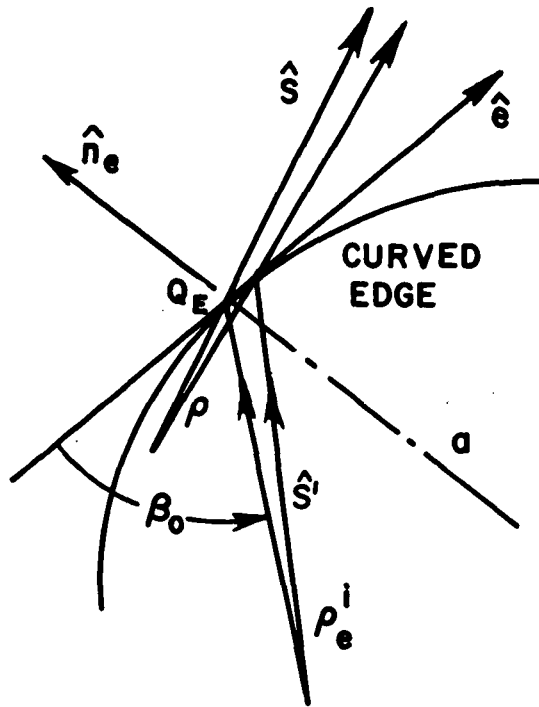


Fig. 4A. Caustic distances associated with the diffraction by a curved edge.

A wavefront is incident on a curved edge at the point  $Q_E$ , where the radius of curvature is  $a$ , the unit tangent vector is  $\hat{e}$ , and the unit normal vector to the edge is  $\hat{n}_e$  given by the Serret-Frenet formula

$$(A-24) \quad \dot{\hat{e}} = -\frac{\hat{n}_e}{a}$$

in which the super dot denotes differentiation with respect to the distance along the edge and  $a$  is taken to be positive. It is apparent from the above equation that  $\hat{n}_e$  is directed away from the center of curvature.

A second useful formula will be derived next. Let  $\bar{r}$  be the position vector from a point 0 to a point on the edge.

$$(A-25) \quad \hat{e} = \frac{\dot{\bar{r}}}{r}$$

$$(A-26) \quad \hat{r} = \bar{r}/r$$

from which

$$(A-27) \quad \dot{\hat{r}} = \frac{\dot{\bar{r}}}{r} - \frac{\bar{r}}{r^2} \dot{r}$$

Since

$$(A-28) \quad r^2 = \bar{r} \cdot \bar{r},$$

$$(A-29) \quad \dot{r} = \dot{\bar{r}} \cdot \hat{r},$$

where Eq. (A-26) has been used.

Substituting Eqs. (A-25), (A-26) and (A-29) into Eq. (A-27) and dot multiplying both sides of the resulting equation by  $\hat{e}$ , one obtains

$$(A-30) \quad \hat{e} \cdot \dot{\hat{r}} = \frac{1 - (\hat{e} \cdot \hat{r})^2}{r}$$

According to Keller's law of edge diffraction,

$$(A-31) \quad \hat{s}' \cdot \hat{e} = \hat{s} \cdot \hat{e} = \cos \beta_0$$

and so

$$(A-32) \quad \hat{s}' \cdot \hat{e} + \hat{e} \cdot \hat{s}' = \hat{s} \cdot \hat{e} + \hat{s} \cdot \hat{e}$$

Employing Eqs. (A-24) and (A-30) in Eq. (A-32)

$$(A-33) \quad \frac{1 - (\hat{e} \cdot \hat{s}')}{\rho_e^i} - \frac{\hat{n}_e \cdot \hat{s}'}{a} = \frac{1 - (\hat{e} \cdot \hat{s})^2}{\rho} - \frac{\hat{n}_e \cdot \hat{s}}{a},$$

where  $\rho_e^i \equiv s'$  is the radius of curvature of the incident wavefront at  $Q_E$  taken in the plane containing the incident ray and  $\hat{e}$ ,

$\rho$  is the caustic distance; it is also the radius of curvature of the diffracted wavefront at  $Q_E$  taken in the plane containing the diffracted ray and  $\hat{e}$ .

Using Eq. (A-31), Eq. (A-33) may be written more compactly as

$$(A-34) \quad \frac{1}{\rho} = \frac{1}{\rho_e^i} - \frac{\hat{n}_e \cdot (\hat{s}' - \hat{s})}{a \sin^2 \beta_0},$$

which has the same form as the elementary lens equation, where  $\rho_e^i$  and  $\rho$  correspond to the source and image distances, respectively. Thus we may write Eq. (A-34) as

$$(A-35) \quad \frac{1}{\rho} = \frac{1}{\rho_e^i} + \frac{1}{f}$$

where  $f$  is interpreted as the focal distance. Eq. (A-34) was first given by Kouyoumjian [8], and it has also appeared in a number of ElectroScience Laboratory reports [34,37]. Recently Deschamps has rederived Eq. (A-34) by a different method [36].

An alternative expression for  $\rho$  has been given by Keller [3]; we will derive it here for the sake of completeness.

From Eq. (A-31)

$$\hat{s} \cdot \hat{e} + \hat{s} \cdot \hat{e} = - \sin \beta_0 \dot{\beta}_0$$

Again using Eqs. (A-25), (A-30) and (A-31)

$$(A-36) \quad \frac{\sin^2 \beta_0}{\rho} - \frac{\hat{n}_e \cdot \hat{d}}{a} = - \sin \beta_0 \dot{\beta}_0$$

$$(A-37) \quad \frac{1}{\rho} = - \frac{\dot{\beta}_0}{\sin \beta_0} + \frac{\cos \delta}{a \sin^2 \beta_0}$$

Here  $\delta$  is the angle between  $\hat{n}_e$  and the diffracted ray.

It has been found more convenient to calculate the edge caustic distance  $\rho$  from Eq. (A-34), which does not contain any derivatives.

Since the edge is a caustic of the diffracted rays, it is clear that one of the principal directions of the diffracted wavefront lies in the plane of diffraction and is perpendicular to the diffracted ray. The other principal direction is perpendicular to the plane of diffraction and is thus tangent to the cone of diffracted rays. At a distance  $s$  from the point  $Q_E$  on the edge the principal radii of curvature of the diffracted wavefront are  $\rho + s$  and  $s$ .

In general the principal directions of the incident and reflected wavefronts associated with rays incident and reflected at  $Q_E$  (recall that these rays lie on the cone of diffracted rays) do not coincide with the principal directions of the diffracted wavefronts associated with rays

diffracted in the directions of incidence and reflection. However in the edge-fixed planes of incidence (or reflection) the curvature of the diffracted and incident (or reflected) wavefronts is the same. The relationship of the diffracted wavefront to the incident wavefront at the shadow boundary is apparent from Eq. (A-34); on the shadow boundary  $\hat{s} = \hat{s}'$  and so  $\rho = \rho_e^i$ . The relationship between the diffracted wavefront and the reflected wavefront on the reflection boundary could be deduced from Eqs. (A-15) and (A-34), but it may be verified more easily in the following way. From Eq. (33) the reflected and diffracted phase functions are the same along the edge, i.e.,

$$\psi^r(Q_E) = \psi^d(Q_E) ;$$

hence

$$\psi^r(Q_E) + s = \psi^d(Q_E) + s$$

in the plane containing the tangent to the edge  $\hat{e}$  and the reflected, diffracted rays at the reflection boundary. It follows that  $\rho = \rho_e^r$ , the radius of curvature of the reflected wavefront in the plane containing the reflected ray and  $\hat{e}$ . The relationships between the radii of curvature of the diffracted wavefront and the incident and reflected wavefronts at the shadow and reflection boundaries described in this paragraph have been noted by Lewis and Boersma [12].

APPENDIX III

THE PLANES OF INCIDENCE AND REFLECTION

In this appendix it will be shown that the angle  $\alpha$  between the edge-fixed plane of reflection and the ordinary plane of incidence is equal to minus the angle between the edge-fixed plane of incidence and the ordinary plane of incidence. We will refer to the ordinary plane of incidence simply as the plane of incidence.

The plane of incidence contains the unit vectors  $\hat{s}'$  and  $\hat{n}$  or  $\hat{s}^r$  and  $\hat{n}$ . The edge-fixed plane of incidence contains the unit vectors  $\hat{s}'$  and  $\hat{e}$ . The edge-fixed plane of reflection contains the unit vectors  $\hat{s}^r$  and  $\hat{e}$ . The plane of incidence and the edge-fixed plane of incidence intersect along the incident ray at  $Q_E$ . The plane of incidence and the edge-fixed plane of reflection intersect along the reflected ray at  $Q_E$ .

Referring to Figs. 2, 5 and 5A and recalling that  $\hat{s}^i = \hat{s}'$  at the edge,

$$(A-38a) \quad \hat{e}_{||}^i = \frac{\hat{s}' \times (\hat{n} \times \hat{s}')}{|\hat{s}' \times (\hat{n} \times \hat{s}')|},$$

$$(A-38b) \quad \hat{\beta}_0^i = \frac{-\hat{s}' \times (\hat{e} \times \hat{s}')}{|\hat{s}' \times (\hat{e} \times \hat{s}')|},$$

$$(A-38c) \quad \hat{e}_{||}^r = \frac{\hat{s}^r \times (\hat{n} \times \hat{s}^r)}{|\hat{s}^r \times (\hat{n} \times \hat{s}^r)|},$$



$$(A-39) \quad \cos \alpha^i = \hat{e}^i \cdot \hat{\beta}'_0 = \frac{(\hat{n} \cdot \hat{s}')(\hat{e} \cdot \hat{s}')}{[1 - (\hat{n} \cdot \hat{s}')^2][1 - (\hat{e} \cdot \hat{s}')^2]}$$

Since  $(\hat{n} \cdot \hat{s}') = -(\hat{n} \cdot \hat{s}^r)$  from the law of reflection and  $(\hat{e} \cdot \hat{s}') = (\hat{e} \cdot \hat{s}^r)$  from the law of edge diffraction, it follows from Eqs. (A-38) and (A-39) that

$$(A-40) \quad \cos \alpha^i = \cos \alpha;$$

hence

$$(A-41) \quad \alpha^i = \pm \alpha.$$

From the definition of angles in Fig. 5A,  $\alpha^i = -\alpha$ .

## APPENDIX IV

### RECIPROCITY

The Lorentz reciprocity theorem imposes an important condition on the solution of an electromagnetic problem. This is a necessary condition and approximate solutions which fail to satisfy it may contain errors which are unacceptably large. We will develop the reciprocity condition for the edge structure under consideration in this report, and see if the high-frequency solutions given in Chapter III satisfy it. Also it will be shown how reciprocity may be used to extend our analysis to a special configuration where it would not be valid if applied directly.

Let the sources  $g$  and  $g'$  radiate in the presence of an edge structure as shown in Fig. 6A; the sources are positioned at a finite distance from the edge and from each other. The surface  $S$  rests on the perfectly-conducting boundary, except in the immediate vicinity of edge, and extends to infinity. The surface  $S_{\infty}$  is the surface at infinity; it joins with  $S$  and together with this surface encloses the region occupied by the sources  $g$  and  $g'$ . The surface  $S$  is sharply rounded at the edge so as to enclose it tightly, but its radius of curvature does not vanish there.

The sources  $g$  and  $g'$  consist of electric and magnetic current moments which may be distributed in a volume, over a surface or along a line, so that the infinitesimal electric current moment

$$(A-42a) \quad d\bar{p}_e = \begin{cases} \bar{J}_v dv, & \text{in a volume} \\ \bar{J}_s ds, & \text{over a surface} \\ I \ell d\ell, & \text{along a line} \end{cases}$$

and the infinitesimal magnetic current moment

$$(A-42b) \quad d\bar{p}_m = \begin{cases} \bar{K}_v dv, & \text{in a volume} \\ \bar{K}_s ds, & \text{over a surface} \\ M \ell d\ell, & \text{along a line} \end{cases}$$

in which  $\bar{J}_v$  is the volume density of electric current,  $\bar{K}_v$  is the volume density of magnetic current, etc. Starting with Maxwell's curl equations in the form

$$(A-43a) \quad \nabla \times \bar{H} - j\omega\epsilon \bar{E} = \frac{d\bar{p}_e}{dv},$$

$$(A-43b) \quad \nabla \times \bar{E} + j\omega\mu \bar{H} = \frac{d\bar{p}_m}{dv},$$

with a little manipulation [38] in which the divergence theorem is employed, one obtains

$$\int_{\text{source } g} (\bar{E}' \cdot d\bar{p}_e - \bar{H}' \cdot d\bar{p}_m) -$$

$$\int_{\text{source } g'} (\bar{E} \cdot d\bar{p}'_e - \bar{H} \cdot d\bar{p}'_m) =$$

$$(A-44) \quad \oint_{S+S_\infty} (\bar{H} \times \bar{E}' - \bar{H}' \times \bar{E}) \cdot \hat{n} ds,$$

where the source  $g'$  and its fields are denoted by primes and the source  $g$  and its fields are the unprimed quantities.

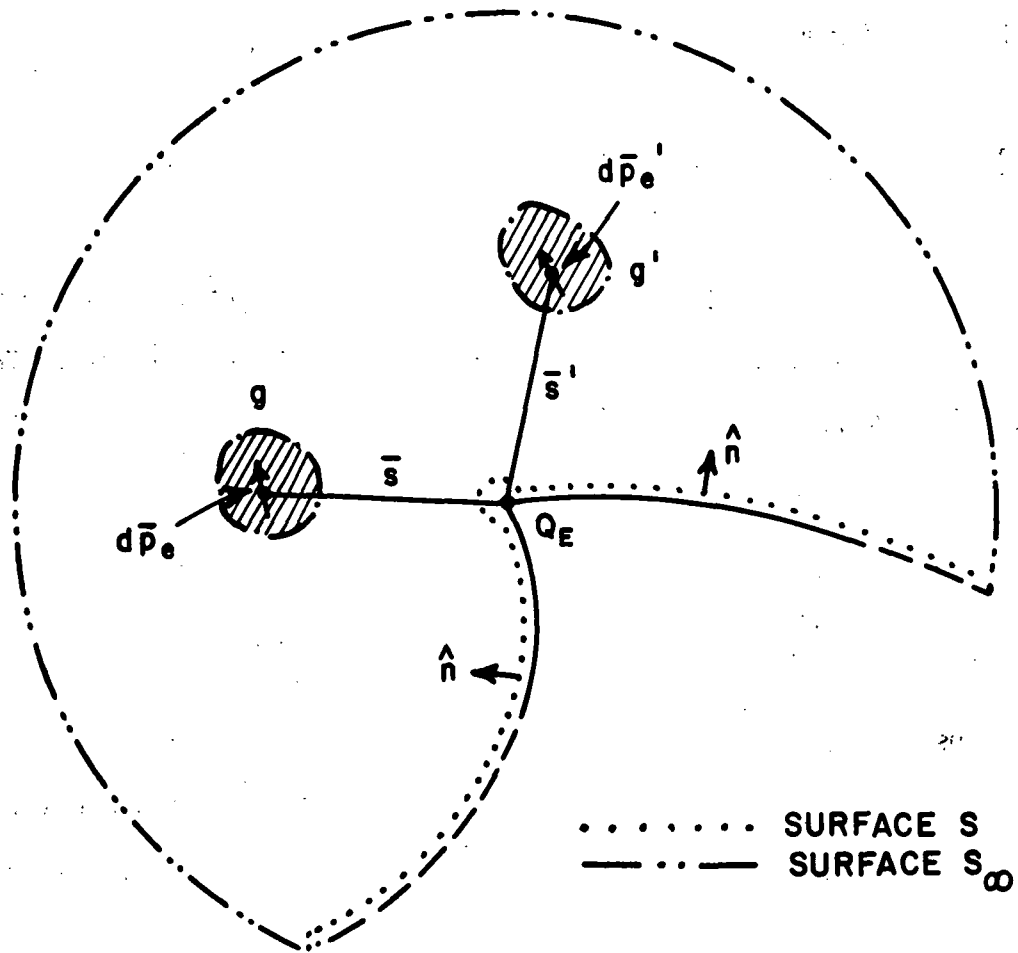


Fig. 6A. Region pertaining to the discussion on the reciprocity principle.

The fields of  $g$  and  $g'$  satisfy an edge condition, also  $\hat{n} \times \bar{E}$ ,  $\hat{n} \times \bar{E}' = 0$  on the boundary surface; hence there is no contribution to the surface integral in Eq. (A-44) from the integration over  $S$ . The fields of  $g$  and  $g'$  also satisfy a radiation condition, so the integration over  $S_\infty$  in Eq. (A-44) vanishes too. Thus

$$(A-45) \quad \int_{\text{source } g} (\bar{E}' \cdot d\bar{p}'_e - \bar{H}' \cdot d\bar{p}'_m) = \int_{\text{source } g'} (\bar{E} \cdot d\bar{p}'_e - \bar{H} \cdot d\bar{p}'_m)$$

which is a statement of reciprocity in integral form. Since the above must be true for any distribution of the sources  $g, g'$ ,

$$(A-46) \quad \bar{E}' \cdot d\bar{p}'_e - \bar{H}' \cdot d\bar{p}'_m = \bar{E} \cdot d\bar{p}'_e - \bar{H} \cdot d\bar{p}'_m$$

It is well known that the geometrical optics field satisfies the reciprocity condition. Since the total field is the sum of the geometrical optics field plus the diffracted field it follows that the diffracted field also satisfies the reciprocity condition; in other words

$$(A-47) \quad \bar{E}^d \cdot d\bar{p}'_e - \bar{H}^d \cdot d\bar{p}'_m = \bar{E}^d \cdot d\bar{p}'_e - \bar{H}^d \cdot d\bar{p}'_m$$

Now let us see if the GTD solution for the diffracted field satisfies Eq. (A-47). We will first consider the reciprocity relationship for a pair of incremental electric current moments  $d\bar{p}'_e, d\bar{p}'_e$ . The electric field of  $d\bar{p}'_e$  incident on the edge is

$$(A-48) \quad \bar{E}^i (Q_E) = \frac{jkz_c}{4\pi} \frac{e^{-jks'}}{s'} \hat{s}' \times (\hat{s}' \times d\bar{p}'_e)$$

$$(A-49) \quad \bar{E}^d \cdot d\bar{p}'_e = \bar{a}' \cdot \bar{D}(\phi, \phi'; \beta_0) \cdot \bar{a} h(s, s')$$

$$(A-50) \quad \bar{E}^d \cdot d\bar{p}'_e = \bar{a} \cdot \bar{D}(\phi', \phi; \beta_0) \cdot \bar{a}' h(s', s)$$

in which

$$(A-51a) \quad \bar{a} = \sqrt{\frac{jkz_c}{4\pi}} d\bar{\rho}_e$$

$$(A-51b) \quad \bar{a}' = \sqrt{\frac{jkz_c}{4\pi}} d\bar{\rho}'_e$$

$$(A-51c) \quad h(s, s') = \frac{1}{s'} \sqrt{\frac{\rho}{s(\rho+s)}} e^{-jk(s+s')},$$

$$(A-51d) \quad h(s', s) = \frac{1}{s} \sqrt{\frac{\rho'}{s'(\rho'+s')}} e^{-jk(s'+s)},$$

$$(A-52a) \quad \frac{1}{\rho} = \frac{1}{s} + \frac{1}{f},$$

$$(A-52b) \quad \frac{1}{\rho'} = \frac{1}{s'} + \frac{1}{f},$$

and

$$(A-53) \quad \frac{1}{f} = - \frac{\hat{n}_e \cdot (\hat{s}' - \hat{s})}{\rho_e \sin^2 \beta}$$

is unchanged when the source and field points are interchanged. Note that the directions of  $\hat{s}'$  and  $\hat{s}$  are reversed when they are interchanged.

Employing Eqs. (A-52) it is seen that

$$\begin{aligned}
 \text{(A-54)} \quad (s'^2 s) \left( \frac{\rho + s}{\rho} \right) &= (s' s)^2 \left( \frac{1}{s} + \frac{1}{\rho} \right) \\
 &= (s s')^2 \left( \frac{1}{s} + \frac{1}{s'} + \frac{1}{f} \right) \\
 &= (s^2 s') \left( \frac{\rho' + s'}{\rho'} \right)
 \end{aligned}$$

From Eqs. (A-51) and (A-54)  $h(s, s')$  has the useful symmetry property

$$\text{(A-55)} \quad h(s, s') = h(s', s) .$$

To satisfy the reciprocity relationship for electric current sources,

$$\text{(A-56)} \quad \bar{E}^{d'} \cdot d\bar{p}_e = \bar{E}^d \cdot d\bar{p}'_e ,$$

it follows from Eqs. (A-49), (A-50), and (A-55) that it is necessary for

$$\text{(A-57)} \quad \bar{a}' \cdot \bar{D}(\phi, \phi'; \beta_0) \cdot \bar{a} = \bar{a} \cdot \bar{D}(\phi', \phi; \beta_0) \cdot \bar{a}' .$$

It is apparent from the form of  $\bar{D}$  in Eqs. (45) and (A-62) that the above is true if

$$\text{(A-58)} \quad D_{\frac{S}{h}}(\phi, \phi'; \beta_0) = D_{\frac{S}{h}}(\phi', \phi; \beta_0) .$$

Consequently, to show that our solution satisfies Eq. (A-56), it is sufficient to show that Eq. (A-58) holds. Furthermore, this is sufficient

to show that the general expression for reciprocity given by Eq. (A-47) is also satisfied, because if Eq. (A-58) is true it can be shown in a manner analogous to the preceding development that  $\bar{H}^{d'} \cdot d\bar{p}_m = \bar{H}^d \cdot d\bar{p}_m'$

We will examine the scalar diffraction coefficients for wedge diffraction first. Referring to Eq. (50), the quantity

$$\cot\left(\frac{\pi^+(\phi+\phi')}{2n}\right) F[kL a^+(\phi+\phi')] + \cot\left(\frac{\pi^+(\phi+\phi')}{2n}\right) F[kL a^-(\phi+\phi')]$$

remains unchanged if  $\phi$  and  $\phi'$  are interchanged. The quantity

$$\cot\left(\frac{\pi^+(\phi-\phi')}{2n}\right) F[kL a^+(\phi-\phi')] + \cot\left(\frac{\pi^-(\phi-\phi')}{2n}\right) F[kL a^-(\phi-\phi')]$$

also remains unchanged, because the two terms are interchanged if  $\phi$  and  $\phi'$  are interchanged. This can be shown by noting that when  $\phi$  and  $\phi'$  are interchanged

$N^+$  is replaced by  $-N^-$ ,

$N^-$  is replaced by  $-N^+$ ,

thus  $a^+(\phi'-\phi) = a^-(\phi-\phi')$ ,

and  $a^-(\phi'-\phi) = a^+(\phi-\phi')$ .

For the sources  $d\bar{p}_e$ ,  $d\bar{p}_e'$

$$(A-59) \quad L = \frac{ss'}{s+s'} \sin^2 \beta_0,$$

so that it is invariant with respect to an interchange of points defined by  $\bar{s}$  and  $\bar{s}'$ .

From the preceding discussion it is clear that the scalar diffraction coefficients for the wedge satisfy Eq. (A-58); hence our GTD solution for the diffraction of an electromagnetic wave by a perfectly-conducting wedge is consistent with reciprocity both within and outside the transition regions.

Turning next to the scalar diffraction coefficients for the curved edge in the curved screen, it is apparent that Eq. (86) is unchanged when  $\phi$  and  $\phi'$  are interchanged. We note that  $L^i$  is invariant with respect to an interchange of source and observation points, because it is given by Eq. (A-59). Thus if the pair of sources are positioned so that they are not in transition regions of each others reflection boundaries,  $F[kL^i a(\phi+\phi')]$  can be replaced by unity, and Eq. (A-58) is satisfied. On the other hand, if the pair of sources  $d\bar{p}_e, d\bar{p}'_e$  are positioned on each other reflection boundaries, the quantities

$$(A-60a) \quad A = \frac{\rho_1^{r+s}}{r \rho_1^s} = \frac{1}{s} + \frac{1}{\rho_1 r} = \frac{1}{s} + \frac{1}{s'} + \frac{1}{f_1}$$

$$(A-60b) \quad B = \frac{\rho_2^{r+s}}{r \rho_2^s} = \frac{1}{s} + \frac{1}{\rho_2 r} = \frac{1}{s} + \frac{1}{s'} + \frac{1}{f_2}$$

$$(A-60c) \quad C = \frac{\rho+s}{\rho s} = \frac{1}{s} + \frac{1}{\rho} = \frac{1}{s} + \frac{1}{s'} + \frac{1}{f}$$

are invariant when  $\bar{s}$  and  $\bar{s}'$  are interchanged. Since

$$(A-61) \quad L^r = \frac{C}{AB} \sin^2 \beta_0,$$

it too must be invariant with respect to this interchange, with the result that Eq. (A-58) is satisfied. Thus we have been able to show that our GTD solution for the diffraction of an electromagnetic wave by a curved screen satisfies the reciprocity condition everywhere except in the transition region of a reflection boundary, and within this region it satisfies the reciprocity condition directly on the boundary itself. It is therefore reasonable to assume that this solution is consistent with reciprocity at all points where it is valid, with the possible exception of some small departures from reciprocity at certain points in the transition region of the reflection boundary.\*

It is pointed out in the text that as  $\phi'$  approaches  $\pi$  and one is close to grazing incidence on the curved screen (see Fig. 11), the solution for the diffraction coefficients given by Eq. (86) becomes invalid, because  $L^r$  approaches 0. However, we may use reciprocity to calculate  $\bar{E}^d(p)$  in the following way. Set  $d\bar{p}_m$  equal to 0 and replace  $d\bar{p}_e$  in Eq. (A-47) by a unit electric current moment  $\hat{u}$  directed parallel to the component of  $\bar{E}^{d'}(p)$  which is to be calculated; then for the incremental sources  $d\bar{p}'_e$  and  $d\bar{p}'_m$  at 0 in Fig. 11

---

\*The solution may satisfy reciprocity at these points, but we have not been able to show it.

$$(A-62) \quad \hat{u} \cdot \bar{E}^{d'}(p) = \frac{-jk}{4\pi} \hat{u} \cdot \left\{ z_c \bar{D}(\phi', \phi; \beta_0) \cdot d\bar{p}'_e - \left[ \bar{D}(\phi', \phi; \beta_0) x s' \right] \cdot d\bar{p}'_m \right\} h(s', s)$$

$$\text{in which } \bar{D}(\phi', \phi; \beta_0) = -\hat{\beta}_0 \hat{\beta}'_0 D_s(\phi', \phi; \beta_0) - \hat{\phi} \hat{\phi}' D_h(\phi', \phi; \beta_0)$$

and  $h(s', s)$  is given by Eq. (A-51d). It is assumed here that  $kL^r$  for incidence from P is sufficiently large so that our approximation for the diffracted field at O is valid. In Eq. (A-62) one would ordinarily let

$$\hat{u} = \begin{cases} \hat{\beta}_0 \\ \hat{\phi} \end{cases}.$$

The discussion of reciprocity for the curved edge in the otherwise smooth, curved surface follows in the same manner as that for the curved edge in the curved screen. One concludes from this that Eq. (89) satisfies Eq. (A-58) for all points at which the scalar diffraction coefficients are valid, except possibly for some points in the transition regions of the shadow boundaries, where small deviations from reciprocity may occur. Also if a problem arises in calculating the diffracted field near grazing incidence on a curved surface ( $\phi' \sim \pi$ ), this calculation may be carried out with the aid of Eq. (A-62).

## REFERENCES

1. J. B. Keller, "The Geometric Optics Theory of Diffraction," presented at the McGill Symposium on Microwave Optics, 1953, Air Force Cambridge Research Center Report TR-59-118 (II), pp. 207-210. 1959.
2. J. B. Keller, "A Geometrical Theory of Diffraction," in Calculus of Variations and its Applications, edited by L. M. Graves, McGraw-Hill Book Co. (1958), pp. 27-52.
3. J. B. Keller, "Geometrical Theory of Diffraction," *J. Opt. Soc. Am.*, 52, pp. 116-130, 1962.
4. M. Kline, "An Asymptotic Solution of Maxwell's Equations," *Comm. Pure and Appl. Math.*, 4, pp. 225-262, 1951.
5. D. L. Hutchins, and R. G. Kouyoumjian, "Asymptotic Series Describing the Diffraction of a Plane Wave by a Wedge," Report 2183-3, 15 December 1969, The Ohio State University ElectroScience Laboratory, Department of Electrical Engineering; prepared under Contract AF 19(628)-5929 for Air Force Cambridge Research Laboratories. (AFCRL-69-0412) (AD 699 228)
6. W. Pauli, "On Asymptotic Series for Functions in the Theory of Diffraction of Light," *phys. Rev.*, 54, pp. 924-931, 1938.
7. F. Oberhettinger, "On asymptotic Series for Functions Occurring in the Theory of Diffraction of Waves by Wedges," *J. Math. Phys.*, 34, pp. 245-255, 1956.
8. P. H. Pathak and R. G. Kouyoumjian, "The Dyadic Diffraction Coefficient for a Perfectly-Conducting Wedge," Report 2183-4, 5 June 1970, The Ohio State University ElectroScience Laboratory,

Department of Electrical Engineering; prepared under Contract  
AF 19(628)-5929 for Air Force Cambridge Research Laboratories.  
(AFCRL-69-0546) (AD 707 827)

9. J. J. Bowman, T. B. A. Senior and P. L. E. Uslenghi,  
Electromagnetic and Acoustic Scattering by Simple Shapes,  
North-Holland Publishing Co., (1969).
10. D. S. Jones, The Theory of Electromagnetism, The Macmillan  
Co. (1964).
11. D. S. Ahluwalia, R. M. Lewis, and J. Boersma, "Uniform  
Asymptotic Theory of Diffraction by a Plane Screen," *SIAM  
J. Appl. Math.*, 16, pp. 783-807, 1968.
12. R. M. Lewis and J. Boersma, "Uniform Asymptotic Theory of  
Edge Diffraction," *J. Math. Phys.*, 10, pp. 2291-2305.
13. D. S. Ahluwalia, "Uniform Asymptotic Theory of Diffraction  
by the Edge of a Three-Dimensional Body," *SIAM J. Appl. Math.*,  
18, pp. 287-301, 1970.
14. J. B. Keller, R. M. Lewis and B. D. Seckler, "Asymptotic  
Solution of Some Diffraction Problems," *Comm. Pure and Appl.  
Math.*, 9, pp. 207-265, 1956.
15. R. G. Kouyoumjian, "Asymptotic High Frequency Methods,"  
*Proc. IEEE*, 53, pp. 864-876, 1965.
16. I. Kay and J. B. Keller, "Asymptotic Evaluation of the Field  
at a Caustic," *J. Appl. Physics*, 25, pp. 876-883, 1954.
17. D. Ludwig, "Uniform Asymptotic Expansions at a Caustic,"  
*Comm. Pure Appl. Math.*, 19, pp. 215-250, 1966.

18. J. B. Keller, "Diffraction by an Aperture," *J. Appl. Physics*, vol. 28, pp. 426-444, April 1957.
19. T. B. A. Senior and P. L. E. Uslenghi, "High-Frequency Backscattering from a Finite Cone," *Radio Sc.*, 6, pp. 393-406, 1971.
20. L. Kaminetsky and J. B. Keller, "Diffraction Coefficients for Higher Order Edges and Vertices," *SIAM J. Appl. Math.*, 22, pp. 109-134, 1972.
21. T. B. A. Senior, "Diffraction Coefficients for a Discontinuity in Curvature," *Electronic Letters*, Vol. 7, No. 10, pp. 249-250, May 20, 1971.
22. T. B. A. Senior, "The Diffraction Matrix for a Discontinuity in Curvature," *IEEE Trans.*, AP-20, pp. 326-333, 1972.
23. P. C. Clemmow, "Some Extensions to the Method of Integration by Steepest Descents," *Quart. J. Mech. and Appl. Math.*, 3, pp. 241-256, 1950.
24. A. Sommerfeld, "Mathematische Theorie der Diffraktion," *Math. Ann.*, 47, pp. 317-374, 1896.
25. R. C. Rudduck, "Application of Wedge Diffraction to Antenna Theory," Report 1691-13, 30 June 1965, The Ohio State University ElectroScience Laboratory, Department of Electrical Engineering; prepared under Grant Number NSG-448 for National Aeronautics and Space Administration. (Available as NASA CR-272, 1965.)

26. Y. Obha, "On the Radiation Patterns of a Corner Reflector," IRE Trans., AP-11, pp. 127-132, 1963.
27. Y. Nomura, "On the Diffraction of Electromagnetic Waves by a Perfectly Reflecting Wedge," Res. Inst. Tohoku University, Japan, Scientific Repts., Series B, vol. 1 and 2, No. 1, pp. 1-24, 1951.
28. C. E. Ryan and L. Peters, Jr., "A Creeping-Wave Analysis of the Edge-On Echo Area of Discs," IEEE Trans., AP-16, pp. 274-275, 1968.
29. T. B. A. Senior, "Disc Scattering at Edge-On Incidence," IEEE Trans., AP-17, pp. 751-756, 1969.
30. R. N. Buchal and J. B. Keller, "Boundary Layer Problems in Diffraction Theory," Comm. Pure Appl. Math., 13, pp. 85-114, 1960.
31. P. Wolfe, "Diffraction of a Scalar Wave by a Plane Screen," J. SIAM Appl. Math., 14, pp. 577-599, 1966.
32. N. Zitron and S. N. Karp, "Higher-Order Approximations in Multiple Scattering. I. Two-Dimensional Scalar Case," J. Math. Physics, 2, pp. 394-4-2, 1961.
33. C. E. Ryan, Jr. and L. Peters, Jr., "Evaluation of Edge-diffracted Fields Including Equivalent Currents for the Caustic Regions," IEEE Trans., AP-17, pp. 292-299, 1969.
34. P. A. J. Ratnasiri, R. G. Kouyoumjian and P. H. Pathak, "The Wide Angle Side Lobes of Reflector Antennas," Report 2183-1, 23 March 1970, The Ohio State University ElectroScience Laboratory, Department of Electrical Engineering; prepared

- under Contract AF 19(628)-5929 for Air Force Cambridge Research Laboratories. (AFCRL-69-0413) (AD 707 105)
35. V. A. Fock, Electromagnetic Diffraction and Propagation Problems, Pergamon Press (1965), Chapt. 8.
  36. G. A. Deschamps, "Ray Techniques in Electromagnetics," Proc. IEEE, 60, pp. 1022-1035, 1972.
  37. C. E. Ryan, Jr., "A Geometrical Theory of Diffraction Analysis of the Radar Cross Section of a Sectionally Continuous Second Degree Surface of Revolution," Report 2430-4, March 1968, The Ohio State University ElectroScience Laboratory, Department of Electrical Engineering; prepared under Contract F-19628-67-C-0318 for Department of the Air Force, Laurence G. Hanscom Field. (AD 669 372)
  38. L. B. Felsen and N. Marcuvitz, Radiation and Scattering of Waves, Prentice-Hall, Inc., (1973), pp. 90-92.

NATIONAL AERONAUTICS AND SPACE ADMINISTRATION  
WASHINGTON, D.C. 20546

OFFICIAL BUSINESS  
PENALTY FOR PRIVATE USE \$300

**SPECIAL FOURTH-CLASS RATE  
BOOK**

POSTAGE AND FEES PAID  
NATIONAL AERONAUTICS AND  
SPACE ADMINISTRATION  
451



POSTMASTER: If Undeliverable (Section 158  
Postal Manual) Do Not Return

*"The aeronautical and space activities of the United States shall be conducted so as to contribute . . . to the expansion of human knowledge of phenomena in the atmosphere and space. The Administration shall provide for the widest practicable and appropriate dissemination of information concerning its activities and the results thereof."*

—NATIONAL AERONAUTICS AND SPACE ACT OF 1958

## NASA SCIENTIFIC AND TECHNICAL PUBLICATIONS

**TECHNICAL REPORTS:** Scientific and technical information considered important, complete, and a lasting contribution to existing knowledge.

**TECHNICAL NOTES:** Information less broad in scope but nevertheless of importance as a contribution to existing knowledge

**TECHNICAL MEMORANDUMS:** Information receiving limited distribution because of preliminary data, security classification, or other reasons. Also includes conference proceedings with either limited or unlimited distribution.

**CONTRACTOR REPORTS:** Scientific and technical information generated under a NASA contract or grant and considered an important contribution to existing knowledge.

**TECHNICAL TRANSLATIONS:** Information published in a foreign language considered to merit NASA distribution in English.

**SPECIAL PUBLICATIONS:** Information derived from or of value to NASA activities. Publications include final reports of major projects, monographs, data compilations, handbooks, sourcebooks, and special bibliographies.

**TECHNOLOGY UTILIZATION PUBLICATIONS:** Information on technology used by NASA that may be of particular interest in commercial and other non-aerospace applications. Publications include Tech Briefs, Technology Utilization Reports and Technology Surveys.

Details on the availability of these publications may be obtained from:

**SCIENTIFIC AND TECHNICAL INFORMATION OFFICE  
NATIONAL AERONAUTICS AND SPACE ADMINISTRATION  
Washington, D.C. 20546**